PROCESS SIMULATION AND CATALYST DEVELOPMENT FOR BIODIESEL PRODUCTION

By

Alex Harris West

B.A.Sc., University of British Columbia, 2003

A THESIS SUBMITTED IN PARTIAL FULFILLMENT OF THE

REQUIREMENTS FOR THE DEGREE OF

MASTER OF APPLIED SCIENCE

in

The Faculty of Graduate Studies

(Chemical and Biological Engineering)

UNIVERSITY OF BRITISH COLUMBIA

August 2006

Abstract

Four continuous biodiesel processes were designed and simulated in HYSYS. The first two employed traditional homogeneous alkali and acid-catalysts. The third and fourth processes used a heterogeneous acid catalyst and a supercritical method, respectively, to convert a waste vegetable oil feedstock into biodiesel. While all processes were capable of producing biodiesel at high purity, the heterogeneous and supercritical processes were the least complex and had the smallest number of unit operations. Material and energy flows, as well as sized unit operation blocks, were used to conduct an economic assessment of each process. Total capital investment, total manufacturing cost and after tax rate-of-return (ATROR) were calculated for each process. The heterogeneous acid catalyst process had the lowest total capital investment and manufacturing costs, and had the only positive ATROR.

Following the results of the process simulations, tin(II) oxide was investigated for use as a heterogeneous catalyst. Unfortunately, catalytic experiments showed no activity. Subsequently, a carbon-based acid catalyst was prepared by sulfonating pyrolysis char, and was studied for its ability to catalyze transesterification of vegetable oil. The catalyst showed only qualitative transesterification, but demonstrated good conversion in free fatty acid esterification. Experiments were designed to measure the effect of alcohol to oil (A:O) molar ratio, reaction time and catalyst loading on the sample. It was observed that free fatty acid (FFA) conversion increased with increasing A:O molar ratio, reaction time and catalyst loading. Conditions that yielded the greatest conversion were 18:1 A:O molar ratio, 3 hour reaction time, 5 wt.% catalyst, 76°C under reflux. The above conditions reduced the FFA content in a waste vegetable oil (WVO)-ethanol mixture from 4.25 wt.% to <0.5 wt.%. Under an 78:1 A:O molar ratio and identical conditions, the catalyst was able to reduce the FFA content of a WVO feedstock from 12.25 wt.% to 1 wt.%. The catalyst has potential to be used in a process converting a high FFA feedstock to biodiesel if the limitations to transesterification can be overcome. Otherwise, it will serve as an excellent catalyst for reducing the FFA content of feedstocks in a two-step acid and base conversion process.

Table of Contents

List of Tables

List of Figures

Nomenclature

Definition	Symbol	Units
After-tax rate of return	$ATROR$	-
Alcohol to oil	$A{:}O$	-
Ammonia	NH_3	-
Auxiliary facility cost	C_{AC}	-
Bare module capital costs	C_{BM}	$
Bare module factor	F_{BM}	-
Bare module factor parameter	B_1	-
Bare module factor parameter	B_2	-
Brunauer, Emmett and Teller	BET	-
Capacity parameter	A	-
Carbon dioxide	CO_2	-
Carboxylic acid group	$COOH$	-
Contingency fee	C_{CF}	$
Energy dispersive X-ray	EDX	-
Fatty acid methyl-ester	$FAME$	-
Fixed capital cost	C_{FC}	$
Free fatty acid	FFA	-
Gas chromatograph	GC	-
Green house gas	GHG	-
Heterogeneous Acid Catalyzed	HAC	-
Materials factor	F_M	-
Non-random two liquid	$NRTL$	-
Pressure factor	F_P	-
Purchase cost	C_p	$
Purchase cost parameter	K_1	-
Purchase cost parameter	K_2	-
Scanning electron microscopy	SEM	-
Sulfate group	SO_4^{2-}	-
Temperature programmed desorption	TPD	-
Thermal conductivity detector	TCD	-
Tin(II) chloride	$SnCl_2$	-
Tin(II) oxide	SnO	-
Total capital investment	C_{TCI}	$
Total manufacturing cost	TMC	$
Total module cost	C_{TM}	$
Waste vegetable oil	WVO	-
Weight per cent	$wt.\%$	-
Working capital cost	C_{WC}	$
X-ray diffraction	XRD	-
X-ray photospectroscopy	XPS	-

Acknowledgements

1 Introduction

Recent concerns over diminishing fossil fuel supplies and rising oil prices, as well as adverse environmental and human health impacts from the use of petroleum fuel have prompted considerable interest in research and development of fuels from renewable resources, such as biodiesel and ethanol. Biodiesel is a very attractive alternative fuel, as it has a number of advantages over conventional diesel fuel. It is derived from a renewable, domestic resource and can therefore reduce reliance on foreign petroleum imports. Biodiesel reduces net carbon dioxide emissions by 78% on a life-cycle basis when compared to conventional diesel fuel (Tyson 2001). It has also been shown to have dramatic improvements on engine exhaust emissions. For instance, combustion of neat biodiesel decreases carbon monoxide (CO) emissions by 46.7%, particulate matter emissions by 66.7% and unburned hydrocarbons by 45.2% (Schumacher et al. 2001). Biodiesel can be used in a regular diesel engine with little to no engine modifications required. Biodiesel is safer to transport due to its higher flash point than diesel fuel. Lastly, biodiesel is biodegradable and non-toxic, making it useful for transportation applications in highly sensitive environments, such as marine ecosystems and mining enclosures. However, biodiesel is not without its disadvantages. These include reduced energy content on per mass basis (this is due to the presence of oxygen in the fuel) which leads to lower power and torque, as well as higher fuel consumption. Additionally, combustion of biodiesel has been shown to cause a slight increase in NO_x formation (Schumacher et al. 2001; Dorado et al. 2003).

As shown in Equation 1.1, biodiesel (defined by the Association for Standards and Testing of Materials as mono-alkyl esters of long chain fatty acids) is usually produced by the transesterification of a lipid feedstock. Transesterification is the reversible reaction of a fat or oil (both of which are composed of triglycerides and free fatty acids) with an alcohol to form fatty acid alkyl esters and glycerol. Stoichiometrically, the reaction requires a 3:1 alcohol:oil (A:O) molar ratio, but because the reaction is reversible, excess alcohol is added to drive the equilibrium toward the products side.

$$
\begin{array}{l}
\text{CH}_2\text{–OOC–R}_1 \\
| \\
\text{CH–OOC–R}_2 \\
| \\
\text{CH}_2\text{–OOC–R}_3
\end{array}
\quad + \quad 3\text{R'OH} \quad \overset{\text{Catalyst}}{\Longleftrightarrow} \quad
\begin{array}{l}
\text{R}_1\text{–COO–R'} \\
\\
\text{R}_2\text{–COO–R'} \\
\\
\text{R}_3\text{–COO–R'}
\end{array}
\quad + \quad
\begin{array}{l}
\text{CH}_2\text{–OH} \\
| \\
\text{CH–OH} \\
| \\
\text{CH}_2\text{–OH}
\end{array}
\qquad (1.1)
$$

| Glyceride | Alcohol | Esters | Glycerol |
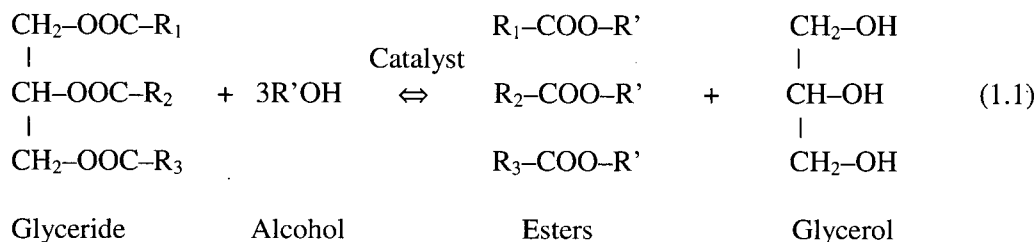
Transesterification can be alkali-, acid- or enzyme-catalyzed; however, enzyme catalysts are rarely used, as they are less effective (Ma and Hanna 1999). The reaction can also take place without the use of a catalyst under conditions in which the alcohol is in a supercritical state (Saka and Kusdiana 2001; Demirbas 2002).

Biodiesel can also be produced by esterification of fatty acid molecules, as shown in Equation 1.2. This reaction can be catalyzed be either a base or an acid or without the use of a catalyst under supercritical conditions (Kusdiana and Saka 2004).
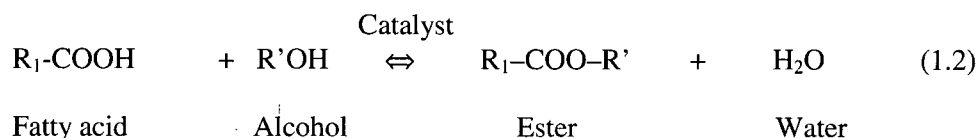
$$
\text{R}_1\text{-COOH} \quad + \quad \text{R'OH} \quad \overset{\text{Catalyst}}{\Longleftrightarrow} \quad \text{R}_1\text{–COO–R'} \quad + \quad \text{H}_2\text{O} \qquad (1.2)
$$

| Fatty acid | Alcohol | Ester | Water |

Currently, the high cost of biodiesel production is the major impediment to its large scale commercialization (Canakci and Van Gerpen 2001). The high cost is largely attributed to the cost of virgin vegetable oil as feedstock, which can account for up to 75% of the final product cost (Krawczyk 1996). Exploring methods to reduce the production cost of biodiesel has been the focus of much recent research. One method involves replacing a virgin oil feedstock with a waste cooking oil feedstock. The costs of waste cooking oil are estimated to be less than half of the cost of virgin vegetable oils (Canakci and Van Gerpen 2001). Furthermore, utilizing waste cooking oil has the advantage of removing a significant amount of material from the waste stream – as of 1990, it was estimated that at least 2 billion pounds of waste grease was produced annually in the United States (Canakci and Van Gerpen 2001).

1.1   Transesterification research

Biodiesel related research has progressed from initial attempts to synthesize the alkyl-ester product through a simple base catalyzed reaction of pure vegetable oil to more sophisticated attempts at bringing production costs down through less expensive feedstocks, different

catalysts (such as homogeneous and heterogeneous acid catalysts) and reaction conditions (such as the reaction of the lipid feedstock with a supercritical alcohol).

1.1.1 Homogeneous alkali-catalyzed transesterification

Transesterification catalyzed by a base such as NaOH or KOH has been extensively studied and reported (Freedman et al. 1984; Noureddini and Zhu 1997; Ma et al. 1998; Komers et al. 2001; Dorado et al. 2002; Dorado et al. 2004) and optimum conditions at atmospheric pressure (60°C, 1 wt.% catalyst, 6:1 A:O molar ratio), are well known (Freedman et al. 1984). Additionally, the kinetics of the reaction have been reported (Freedman et al. 1986; Noureddini and Zhu 1997) as following a second order reaction mechanism, through two distinct reaction phases. The reaction rate is initially controlled by mass transfer between the alcohol and oil phases, and is then controlled by kinetic limitations as it approaches equilibrium.

In order to prevent saponification (soap formation) during the reaction which leads to difficulty during downstream purification, the free fatty acid (FFA) and water content of the feed must be below 0.5 wt.% and 0.05 wt.%, respectively (Freedman et al. 1984). Because of these limitations, only pure vegetable oil feeds are appropriate for alkali-catalyzed transesterification without extensive pretreatment.

1.1.2 Homogeneous acid-catalyzed transesterification

A homogeneous acid-catalyzed process can be employed to take advantage of cheaper feedstocks, such as waste cooking oil and animal-based tallow. The acid-catalyzed process can tolerate up to 5 wt.% FFA, but is sensitive to water content greater than 0.5 wt.%. The disadvantage of this method is that it is extremely slow at mild conditions: Canakci and Van Gerpen (1999), found that it took 48 hours to achieve a 98% conversion at 60°C at an A:O molar ratio of 30:1 which are typical conditions for this reaction. At higher temperatures and pressures (e.g. 100°C and 3.5 bar) reaction times can be substantially reduced (down to 8 h) to achieve 99% conversion (Goff et al. 2004).

Kinetic studies of the homogeneous acid-catalyzed reaction have been scarce compared to the base-catalyzed reaction. Freedman et al. (1986) investigated the acid catalyzed transesterification of soybean oil with butanol at 60°C. At a 30:1 A:O molar ratio and 1 wt.%

catalyst loading, the forward reactions were observed to be pseudo-first order with the overall reaction occurring as a series of consecutive reactions.

1.1.3 Heterogeneously catalyzed transesterification

A process employing a heterogeneous catalyst is appealing because the ease of catalyst separation from the product stream provides an advantage over the traditional homogeneous processes. To this end, significant effort has been expended to identify and screen heterogeneous catalysts that have high potential for biodiesel production.

1.1.3.1 Solid base catalysts

Several researchers have investigated the transesterification properties of solid base catalysts. Kim et al. (2004) found that a yield of 78% could be achieved after 2 hours using Na/NaOH/γ-Al2O3 as a catalyst, at 60°C, 1 atm and 6:1 A:O molar ratio. Increased yield of 90% was achieved by the addition of a cosolvent, n-hexane, with the A:O molar ratio of 9:1. Gryglewicz (1999) reported that after 2.5 hours at 60°C and 4.5:1 A:O molar ratio, calcium oxide or calcium methoxide as catalyst gave biodiesel yields of 90%. However, no reports exist demonstrating the ability of solid base catalysts to esterify FFAs present in waste vegetable oil and animal tallow.

1.1.3.2 Solid acid catalysts

Due to their ability to catalyze both esterification and transesterification reactions, a large number of heterogeneous acid catalysts including solid metal oxides and zeolytes have been screened for activity as summarized in Table 1 (Furuta et al. 2004; Lopez et al. 2005; Jitputti et al. 2006).

Extensive work has also gone into developing and testing catalysts for esterification of free fatty acids. Mbaraka and Shanks (2005) designed a mesoporous silica catalyst (MCM-41) with specially tailored hydrophobic groups to prevent catalyst deactivation by the water produced during the esterification reaction. Furuta et al. (2004) tested their catalysts for esterification activity, and reported that conversions of 100% were achieved at a temperature of 200°C in the esterification of n-octanoic acid with methanol. Toda et al. (2005) recently developed an acid catalyst by adding sulfonite groups to a carbon skeleton obtained by pyrolyzing refined sugar. Catalyst activity was more than half that of the conventional homogeneous acid reaction, and

greater than that of other solid acid catalysts; however, the yield of the process was not mentioned.

Research concerning heterogeneous catalysts is still in the catalyst screening stage. Studies regarding reaction kinetics, as well as improving reaction parameters have yet to be conducted. In addition, studies to determine the effects of free fatty acid concentration and water on the performance of the catalyst have been scarce.

Table 1.1. Selected heterogeneous acid catalysts used for transesterification of triglycerides and their results.

Reference	Catalyst Type	Feedstock	Molar ratio	Temperature (°C)	Pressure (atm)	Time (min)	Conversion Achieved (%)
(Furuta et al. 2004)	Tungstated zirconia	SBO*	40	300	1		90
	Sulfated zirconia	SBO	40	300	1		80
	Sulfated tin oxide	SBO	40	300	1		68
(Jitputti et al. 2006)	Sulfated zirconia	Palm kernel oil	6	200	40.5		90.3
	Zinc oxide	Palm kernel oil	6	200	40.5		86.1
	Sulfated tin dioxide	Palm kernel oil	6	200	40.5		90.3
	KNO$_3$/KL zeolyte	Palm kernel oil	6	200	40.5		71.4
(Lopez et al. 2005)	Amberlyst-15	Triacetin	6	60	1	480	79
	Nafion NR50	Triacetin	6	60	1	480	33
	Sulfated zirconia	Triacetin	6	60	1	480	57
	Tungstated zirconia	Triacetin	6	60	1	480	10
	Zeolyte Hβ	Triacetin	6	60	1	480	<10
	ETS-10 (H)	Triacetin	6	60	1	480	<10

*Soybean oil

1.1.4 Supercritical transesterification

Supercritical transesterification is also a potential alternative to the standard homogenous catalytic routes. Transesterification using supercritical methanol has been shown to give nearly complete conversion in small amount of time (15 minutes) (Warabi et al. 2004). High

temperatures, (up to 350°C) and large A:O ratios (42:1) are required to achieve the high levels of conversion that have been reported (Kusdiana and Saka 2001). In addition to the high conversion and reaction rates, supercritical transesterification is appealing as it can tolerate feedstocks with very high contents of FFAs and water, up to 36 wt.% and 30 wt.%, respectively (Kusdiana and Saka 2004).

1.2 Process modelling and economic assessment

Another important tool for addressing the economic aspects of biodiesel is process modelling. Process modelling can be used to investigate the effect of process variables, such as plant scale, raw material costs, utility costs, product selling prices etc. on the economic feasibility of the process. Bender (1999) conducted a review of economic feasibility studies from different feedstocks such as beef tallow and canola seed oil. However, these studies are limited to processes employing an alkali-catalyzed reaction.

More recently, Zhang et al. (2003a) developed a series of HYSYS based process simulations to assess the technological feasibility of four different biodiesel plant configurations – a homogeneous alkali-catalyzed pure vegetable oil process; a two-step process to treat waste vegetable oil; a single step homogeneous acid-catalyzed process to treat waste vegetable oil; and a homogeneous acid-catalyzed process using hexane extraction to purify the biodiesel. All four configurations were deemed technologically feasible (i.e., they were capable of producing biodiesel to meet the ASTM specification for purity, 99.65 wt.%), but a subsequent economic analysis of the four designs revealed that the one step acid-catalyzed process was the most economically attractive process (Zhang et al. 2003b). Haas et al. (2006) developed a process simulation model to estimate the costs of biodiesel production. The model was capable of predicting the effect on production cost given fluctuations in feedstock cost or product selling price. The model was also designed to calculate the effects on capital cost and production cost upon modification of the process, such as changes in feedstock type and cost, and process chemistry and technology. However, the model was limited to the traditional alkali-catalyzed production method.

1.3 Thesis objectives

In order to determine whether the supercritical methanol or the heterogeneous acid catalyst process is a promising alternative to the standard homogeneous catalytic routes, the aim of Part I

of this thesis is to develop a process flowsheet and simulation, conduct an economic analysis of each process based on the material and energy balance results reported by HYSYS, and carry out sensitivity analyses to optimize each process. Additionally, the sizing and economic calculations are incorporated into each simulation by way of the spreadsheet tool available in HYSYS. The material and energy flows, as well as some unit parameters are imported directly into the spreadsheet, thereby allowing the sizing and economic results to be updated automatically when any changes were made to the process flowsheet.

Based on the outcome of the process simulations, it was desired to conduct more detailed catalytic studies of the heterogeneous catalyst. Therefore Part II of this thesis has investigated the synthesis and characterization of a heterogeneous catalyst, as well as testing its activity with respect to transesterification, investigating the effects reaction time, A:O molar ratio and catalyst loading on the outcome of the reaction, and the effects of free fatty acid content in the reaction mixture.

1.4   Thesis format

The remainder of this thesis continues with two manuscripts. Chapter 2 reports the results on the design and assessment of four biodiesel production processes using HYSYS.Plant (submitted for publication in Bioresource Technology). Chapter 3 concentrates on the synthesis and testing of a new heterogeneous catalyst (in preparation for submission). Finally, the thesis is concluded in Chapter 4 with a general discussion of the results and recommendations for further research. References are presented at the end of each chapter.

1.5 References

Bender, M. (1999). Economic feasibility review for community-scale farmer cooperatives for biodiesel. Bioresource Technology 70(1): 81-87.

Canakci, M. and Van Gerpen, J. (1999). Biodiesel production via acid catalysis. Transactions of the ASAE 42(5): 1203-1210.

Canakci, M. and Van Gerpen, J. (2001). Biodiesel production from oils and fats with high free fatty acids. Transactions of the ASAE 44(6): 1429-1436.

Demirbas, A. (2002). Biodiesel from vegetable oils via transesterification in supercritical methanol. Energy Conversion and Management 43(17): 2349-2356.

Dorado, M. P., Ballesteros, E., Arnal, J. M., Gomez, J. and Gimenez, F. J. L. (2003). Testing waste olive oil methyl ester as a fuel in a diesel engine. Energy & Fuels 17(6): 1560-1565.

Dorado, M. P., Ballesteros, E., de Almeida, J. A., Schellert, C., Lohrlein, H. P. and Krause, R. (2002). An alkali-catalyzed transesterification process for high free fatty acid waste oils. Transactions of the ASAE 45(3): 525-529.

Dorado, M. P., Ballesteros, E., Mittelbach, M. and Lopez, F. J. (2004). Kinetic parameters affecting the alkali-catalyzed transesterification process of used olive oil. Energy & Fuels 18(5): 1457-1462.

Freedman, B., Butterfield, R. O. and Pryde, E. H. (1986). Transesterification kinetics of soybean oil. Journal of the American Oil Chemists Society 63(10): 1375-1380.

Freedman, B., Pryde, E. H. and Mounts, T. L. (1984). Variables affecting the yields of fatty esters from transesterified vegetable-oils. Journal of the American Oil Chemists Society 61(10): 1638-1643.

Furuta, S., Matsuhashi, H. and Arata, K. (2004). Biodiesel fuel production with solid superacid catalysis in fixed bed reactor under atmospheric pressure. Catalysis Communications 5(12): 721-723.

Goff, M. J., Bauer, N. S., Lopes, S., Sutterlin, W. R. and Suppes, G. J. (2004). Acid-catalyzed alcoholysis of soybean oil. Journal of the American Oil Chemists Society 81(4): 415-420.

Gryglewicz, S. (1999). Rapeseed oil methyl esters preparation using heterogeneous catalysts. Bioresource Technology 70(3): 249-253.

Haas, M. J., McAloon, A. J., Yee, W. C. and Foglia, T. A. (2006). A process model to estimate biodiesel production costs. Bioresource Technology 97(4): 671-678.

Jitputti, J., Kitiyanan, B., Rangsunvigit, P., Bunyakiat, K., Attanatho, L. and Jenvanitpanjakul, P. (2006). Transesterification of crude palm kernel oil and crude coconut oil by different solid catalysts. Chemical Engineering Journal 116(1): 61-66.

Kim, H. J., Kang, B. S., Kim, M. J., Park, Y. M., Kim, D. K., Lee, J. S. and Lee, K. Y. (2004). Transesterification of vegetable oil to biodiesel using heterogeneous base catalyst. Catalysis Today 93-95: 315-320.

Komers, K., Machek, J. and Stloukal, R. (2001). Biodiesel from rapeseed oil, methanol and KOH 2. Composition of solution of KOH in methanol as reaction partner of oil. European Journal of Lipid Science and Technology 103(6): 359-362.

Krawczyk, T. (1996). Biodiesel. INFORM 7(8): 801-822.

Kusdiana, D. and Saka, S. (2001). Kinetics of transesterification in rapeseed oil to biodiesel fuel as treated in supercritical methanol. Fuel 80(5): 693-698.

Kusdiana, D. and Saka, S. (2004). Effects of water on biodiesel fuel production by supercritical methanol treatment. Bioresource Technology 91(3): 289-295.

Lopez, D. E., Goodwin, J. G., Bruce, D. A. and Lotero, E. (2005). Transesterification of triacetin with methanol on solid acid and base catalysts. Applied Catalysis, A: General 295(2): 97-105.

Ma, F., Clements, L. D. and Hanna, M. A. (1998). The effects of catalyst, free fatty acids, and water on transesterification of beef tallow. Transactions of the ASAE 41(5): 1261-1264.

Ma, F. R. and Hanna, M. A. (1999). Biodiesel production: A review. Bioresource Technology 70(1): 1-15.

Mbaraka, I. K. and Shanks, B. H. (2005). Design of multifunctionalized mesoporous silicas for esterification of fatty acid. Journal of Catalysis 229(2): 365-373.

Noureddini, H. and Zhu, D. (1997). Kinetics of transesterification of soybean oil. Journal of the American Oil Chemists Society 74(11): 1457-1463.

Saka, S. and Kusdiana, D. (2001). Biodiesel fuel from rapeseed oil as prepared in supercritical methanol. Fuel 80(2): 225-231.

Schumacher, L. G., Marshall, W., Krahl, J., Wetherell, W. B. and Grabowski, M. S. (2001). Biodiesel emissions data from series 60 ddc engines. Transactions of the ASAE 44(6): 1465-1468.

Toda, M., Takagaki, A., Okamura, M., Kondo, J. N., Hayashi, S., Domen, K. and Hara, M. (2005). Green chemistry: Biodiesel made with sugar catalyst. Nature 438(7065): 178.

Tyson, K. S. Biodiesel: Handling and use guidelines. http://www.eere.energy.gov/biomass/pdfs/biodiesel_handling.pdf (November 28, 2004),

Warabi, Y., Kusdiana, D. and Saka, S. (2004). Reactivity of triglycerides and fatty acids of rapeseed oil in supercritical alcohols. Bioresource Technology 91(3): 283-287.

Zhang, Y., Dube, M. A., McLean, D. D. and Kates, M. (2003a). Biodiesel production from waste cooking oil: 1. Process design and technological assessment. Bioresource Technology 89(1): 1-16.

Zhang, Y., Dube, M. A., McLean, D. D. and Kates, M. (2003b). Biodiesel production from waste cooking oil: 2. Economic assessment and sensitivity analysis. Bioresource Technology 90(3): 229-240.

2 Assessment of Four Continuous Biodiesel Production Processes using HYSYS.Plant[1]

2.1 Introduction and background

Recent concerns over diminishing fossil fuel supplies and rising oil prices, as well as adverse environmental and human health impacts from the use of petroleum fuel have prompted considerable interest in research and development of fuels from renewable resources, such as biodiesel and ethanol. Biodiesel is a very attractive alternative fuel, as it is derived from a renewable, domestic resource and can therefore reduce reliance on foreign petroleum imports. Biodiesel reduces net carbon dioxide emissions by 78% on a life-cycle basis when compared to conventional diesel fuel (Tyson 2001). It has also been shown to have dramatic improvements on engine exhaust emissions. For instance, combustion of neat biodiesel decreases carbon monoxide (CO) emissions by 46.7%, particulate matter emissions by 66.7% and unburned hydrocarbons by 45.2% (Schumacher et al. 2001). Additionally, biodiesel is biodegradable and non-toxic, making it useful for transportation applications in highly sensitive environments, such as marine ecosystems and mining enclosures.

As shown in Equation 2.1, biodiesel (alkyl ester) is usually produced by the transesterification of a lipid feedstock. Transesterification is the reversible reaction of a fat or oil (both of which are composed of triglycerides and free fatty acids) with an alcohol to form fatty acid alkyl esters and glycerol. Stoichiometrically, the reaction requires a 3:1 molar A:O ratio, but because the reaction is reversible, excess alcohol is added to drive the equilibrium toward the products side.

$$
\begin{array}{llll}
CH_2-OOC-R_1 & & R_1-COO-R' & CH_2-OH \\
| & \text{Catalyst} & | \\
CH-OOC-R_2 & + 3R'OH \Leftrightarrow & R_2-COO-R' & + & CH-OH & \quad (2.1) \\
| & & & | \\
CH_2-OOC-R_3 & & R_3-COO-R' & CH_2-OH
\end{array}
$$

Glyceride   Alcohol   Esters   Glycerol
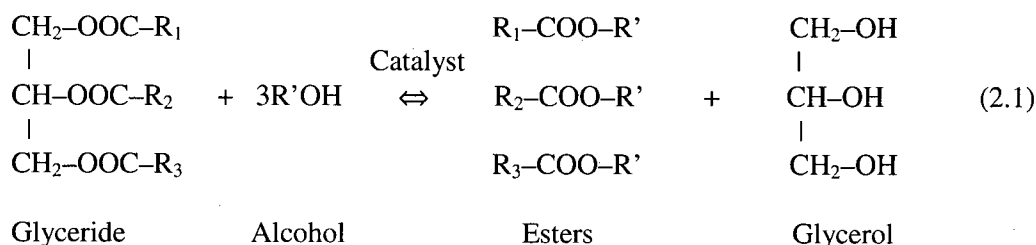
Transesterification can be alkali-, acid- or enzyme-catalyzed; however, enzyme catalysts are rarely used, as they are less effective (Ma and Hanna 1999). The reaction can also take place without the use of a catalyst under conditions in which the alcohol is in a supercritical state (Saka and Kusdiana 2001; Demirbas 2002).

---

[1] A version of this chapter has been submitted for publication. West, A.H., Posarac, D. and Ellis, N. (2006) Assessment of Four Continuous Biodiesel Production Processes using HYSYS.Plant. Bioresource Technology.

Currently, the high cost of biodiesel production is the major impediment to its large scale commercialization (Canakci and Van Gerpen 2001). The high cost is largely attributed to the cost of virgin vegetable oil as feedstock. Exploring methods to reduce the production cost of biodiesel has been the focus of much recent research. One method involves replacing a virgin oil feedstock with a waste cooking oil feedstock. The costs of waste cooking oil are estimated to be less than half of the cost of virgin vegetable oils (Canakci and Van Gerpen 2001). Furthermore, utilizing waste cooking oil has the advantage of removing a significant amount of material from the waste stream – as of 1990, it was estimated that at least 2 billion pounds of waste grease was produced annually in the United States (Canakci and Van Gerpen 2001).

In the last few years, a number of new production methods have emerged from laboratory/bench-scale research aimed at reducing the cost of biodiesel (Demirbas 2002; Canakci and Van Gerpen 2003; Delfort et. al. 2003). One such method uses alcohol in its supercritical state, and eliminates the need for a catalyst. Additionally, the supercritical process requires only a short residence time to reach high conversion (Kusdiana and Saka 2004). Another option is to use a solid catalyst to catalyze the reaction (Furuta et al. 2004; Suppes et al. 2004; Abreu et al. 2005). Use of a solid phase catalyst to produce biodiesel will simplify downstream purification of the biodiesel. The catalyst can be separated by physical methods such as a hydrocyclone in the case where a multiphase reactor is used. Alternatively, a fixed bed reactor would eliminate the catalyst removal step entirely.

Zhang et al. (2003a) developed a HYSYS based process simulation model to assess the technological feasibility of four biodiesel plant configurations – a homogeneous alkali-catalyzed pure vegetable oil process; a two-step process to treat waste vegetable oil; a single step homogeneous acid-catalyzed process to treat waste vegetable oil; and a homogeneous acid-catalyzed process using hexane extraction to help purify the biodiesel. All four configurations were deemed technologically feasible, but a subsequent economic analysis of the four designs revealed that the one step acid-catalyzed process was the most economically attractive process Zhang et al. (2003b). Haas et al. (2006) developed a versatile process simulation model to estimate biodiesel production costs; however, the model was limited to a traditional alkali-catalyzed production method. In order to determine whether the supercritical methanol or the heterogeneous acid catalyst process is a promising alternative to the standard homogeneous

11

catalytic routes, our aim is to develop a process flowsheet and simulation, conduct an economic analysis of each process based on the material and energy balance results reported by HYSYS, and carry out sensitivity analyses to optimize each process. Additionally, it was desired to automate the sizing and economic calculations, whence they were incorporated into each simulation by way of the spreadsheet tool available in HYSYS. The material and energy flows, as well as some unit parameters were imported directly into the spreadsheet, thereby allowing the sizing and economic results to be updated automatically when any changes were made to the process flowsheet. Additional comparison is made to the simulation work by Zhang et al. (2003a) in order to ensure that the present simulations provide comparable results.

The homogeneous alkali-catalyzed system has been well studied, and optimum conditions at 1 atm pressure (60°C, 1 wt.% catalyst, 6:1 A:O molar ratio), are known (Freedman et al. 1984). In order to prevent saponification during the reaction, the free fatty acid (FFA) and water content of the feed must be below 0.5 wt.% and 0.05 wt.%, respectively (Freedman et al. 1984). Because of these limitations, only pure vegetable oil feeds are appropriate for alkali-catalyzed transesterification without extensive pretreatment.

A homogeneous acid-catalyzed process can be employed to take advantage of cheaper feedstocks, such as waste cooking oil and animal-based tallow. The acid-catalyzed process can tolerate up to 5 wt.% FFA, but is sensitive to water content greater than 0.5 wt.%. The disadvantage of this method is that it is extremely slow at mild conditions: Canakci and Van Gerpen (1999) found that it took 48 hours to achieve a 98% conversion at 60°C at an A:O ratio of 30:1. At higher temperatures and pressures (e.g. 100°C and 3.5 bar) reaction times can be substantially reduced (down to 8 h) to achieve similar a degree of (99%) conversion (Goff et al. 2004).

A process using a heterogeneous acid-catalyst is appealing because of the ease of separation of a solid catalyst. Lotero et al. (2005) reports this advantage, coupled with the ability of the acid functionality to process low cost, high free fatty acid feedstocks, will yield the most economical biodiesel production method. As outlined in Table 2.1, a number of solid phase catalysts have been identified that hold potential for use. Research concerning heterogeneous catalysts is still in the catalyst screening stage. Studies regarding reaction kinetics, as well as improving reaction

parameters have yet to be conducted. In addition, studies to determine the effects of free fatty acid concentration and water on the performance of the catalyst have been scarce.

Supercritical transesterification is also a potential alternative to the standard homogenous catalytic routes. Supercritical transesterification using methanol has been shown to give nearly complete conversion in a relatively short period (15 minutes) (Warabi et al. 2004). High temperatures, (up to 350°C) and large A:O ratios (42:1) are required to achieve the high levels of conversion (Kusdiana and Saka 2001). In addition to the high conversion and reaction rates, supercritical transesterification is appealing as it can tolerate feedstocks with very high contents of FFAs and water, up to 36 wt.% and 30 wt.%, respectively (Kusdiana and Saka 2004).

2.2 Process simulation

To assess the technological feasibility and obtain material and energy balances for a preliminary economic analysis, complete process simulations were performed. Despite some expected differences between a process simulation and real-life operation, process simulators are commonly used to provide reliable information on process operation, owing to their vast component libraries, comprehensive thermodynamic packages and advanced computational methods. HYSYS Plant NetVer 3.2 was used to conduct the simulation. HYSYS was selected as a process simulator for both its simulation capabilities and the ability to easily incorporate sizing and economic calculations within the spreadsheet tool. The first steps in developing the process simulation were selecting the chemical components for the process, as well as a thermodynamic model. Additionally, unit operations and operating conditions, plant capacity and input conditions must all be selected and specified. The unit operations, plant capacity and input conditions for the base cases, i.e., homogeneous acid and alkali-catalyzed processes, as well as distillation column operating conditions, were selected based on the research done by Zhang et al. (2003a) to ensure that each of the four processes simulated in this work could be compared in a consistent manner.

The HYSYS library contained information for the following components used in the simulation: methanol, glycerol, sulfuric acid, sodium hydroxide, and water. Canola oil was selected as the feedstock, and represented by triolein, as oleic acid is the major fatty acid in canola oil. Accordingly, methyl-oleate, available in the HYSYS component library, was taken as the product of the transesterification reaction. Where a simulation required a feedstock with some

amount of free fatty acids, oleic acid, also available in the HYSYS library, was specified as the free fatty acid present.

Components not available in the HYSYS library were specified using the "Hypo Manager" tool. Calcium oxide, calcium sulfate, phosphoric acid, sodium phosphate and triolein were all specified in this manner. Specification of a component requires input of a number of properties, such as normal boiling point, density, molecular weight, as well as the critical properties of the substance. Since triolein is a crucial component and is involved in operations requiring data for liquid and vapour equilibria, great care was taken in specifying the values as accurately as possible. Values for density, boiling point and critical temperature, pressure and volume were obtained from the ASPEN Plus component library and were input as 915 kg/m^3, 846°C, 1366°C, 470 kPa, 3.09 m^3/kmol, respectively. Additionally, the UNIFAC structure for triolein was specified in order to provide binary interaction parameter estimates.

Owing to the presence of polar compounds such as methanol and glycerol in the process, the non-random two liquid (NRTL) thermodynamic/activity model was selected for use as the property package for the simulation. Some binary interaction parameter coefficients (such as the methanol-methyl oleate coefficient) were unavailable in the simulation databanks, and were estimated using the UNIFAC vapour-liquid equilibrium and UNIFAC liquid-liquid equilibrium models where appropriate.

Plant capacity was specified at 8000 metric tonnes/yr biodiesel (Zhang et al. 2003a). This translated to vegetable oil feeds of roughly 1000 kg/h for each process configuration.

The process units common to all configurations include reactors, distillation columns, pumps and heat exchangers. The homogeneous acid- and alkali-catalyzed processes included liquid-liquid extraction columns to separate the catalyst and glycerol from the biodiesel. In contrast to the base case scenarios, a gravity separation unit was included in the supercritical methanol and heterogeneous acid catalyst processes. In spite of the availability of kinetic data for the alkali-catalyzed, homogeneous acid-catalyzed and, supercritical processes (Freedman et al. 1986; Kusdiana and Saka 2001), the reactors were modeled as conversion reactors since kinetic information for the heterogeneous acid-catalyzed process was unavailable. The reactors were

14

assumed to operate continuously for all cases. Lab-scale reaction conditions and conversion data were available for all processes, assumed to be appropriate for large-scale production, and set as the operating conditions for each reactor. The following conversions were assumed for each process: 97 %, 97%, 94% and 98% for the alkali, acid, heterogeneous and supercritical cases, respectively (Zhang et al. 2003a; Warabi et al. 2004; Abreu et al. 2005). The mono- and di-glyceride intermediates were neglected during the reaction (Zhang et al. 2003a).

Multi-stage distillation was used to recover the excess methanol, as well as in the final purification of biodiesel. Distillation columns were specified to meet or exceed the ASTM standard for biodiesel purity, i.e., 99.65 wt.%. Reflux ratios for the heterogeneous acid-catalyzed and supercritical cases were calculated by determining the minimum reflux ratio using a shortcut distillation column, and then multiplying by 1.5 to obtain the optimum reflux ratio (McCabe et al. 2001). The methanol recovery columns were able to operate at ambient pressures (except in the alkali-catalyzed case), while vacuum operation in the methyl-ester purification columns was necessary to keep the temperatures of the distillate and bottoms streams at suitably low levels, as biodiesel and glycerol are subject to degradation at temperatures greater than 250°C and 150°C, respectively (Newman 1968; Goodrum 2002).

2.3 Process design

Four continuous processes were simulated. Two were based on an alkali-catalyzed transesterification process using virgin vegetable oil (Process I), and a homogeneous acid-catalyzed process using a waste cooking oil feedstock, containing 5 wt.% free fatty acids (Process II). The third configuration employed a heterogeneous acid-catalyst (HAC), tin(II) oxide, in a multiphase reactor fed with waste vegetable oil (Process III), while the final process used a supercritical (SC) methanol treatment of waste vegetable oil to produce biodiesel (Process IV). Process flowsheets are presented in Figures 2.1 to 2.4.

The processes all followed the same general scheme. The vegetable oil was transesterified in the first step, and then sent for downstream purification. Downstream purification consisted of the following steps: methanol recovery by distillation; catalyst neutralization; glycerol separation and catalyst removal; and methyl-ester purification by distillation. Table 2.2 gives details for the

15

unit operations in each process. Tables 2.3 to 2.6 present the feed and product material flow details for each process.

As illustrated in Table 2.1, there are a number of key differences between the processes. The first difference is with regards to the catalyst removal method. The solid catalyst in Process III is removed by a hydrocyclone before methanol recovery, whereas the liquid phase catalyst in processes I is removed by washing the product stream with water in a liquid-liquid extraction column. The acid catalyst in Process II was removed as a solid precipitate in separator X-100 after neutralization in reactor CRV-101. As in the homogeneous acid-catalyst process, the alkali-catalyst had to be neutralized before it could be disposed of. The heterogeneous catalyst in Process III required no neutralization step; it was discarded as a waste product. However, a heterogeneous catalyst has the potential advantage of being recycled.

The second major difference is in the separation of glycerol from the biodiesel. In Processes I and II, glycerol is removed by washing the product stream with water, and collected in the bottoms product. In Processes III and IV, glycerol is separated from the biodiesel in a three-phase separator by gravity settling. Krawczyk (1996) initially proposed gravity separation to remove glycerol; however, Zhang et al. (2003a) indicated from their simulation that satisfactory separation could not be achieved by gravity alone. In the present work, gravity separation was used to separate the biodiesel from the glycerol, and a satisfactory separation was achieved. Note, however, that the calculations for this unit operation are based on parameters that have been estimated by HYSYS and therefore may not truly represent a real system. Additional experimental data are needed to verify the applicability and results of the gravity separator, in order to use the unit block with confidence. In practice, a gravity separation unit has been used on a pilot plant scale to separate glycerol and biodiesel (Canakci and Van Gerpen 2003). All processes produced biodiesel at a higher purity than required by the ASTM standard of 99.65 wt.%.

2.4 Equipment sizing

Process equipment was sized according to principles outlined in Turton et al. (2003) and Seider et al. (2003). The principal dimensions of each unit are presented in Table 2.7. The equipment sizing calculations were conducted using the Spreadsheet tool available within HYSYS. Key variables for unit sizing were imported from the flowsheet directly to the spreadsheet. Sizing

16

equations were encoded within the spreadsheet. Therefore any alterations to the flowsheet, such as component fractions, component flowrates, changes to the desired recovery in the distillations columns, etc. are automatically calculated and implemented, thus eliminating tedious recalculation steps.

2.4.1 Reactor vessels

Reactors were sized for continuous operation by dividing the residence time requirement by the feed flowrate for each process. Residence times were: 4 hours, 4 hours, 3 hours and 20 minutes for the alkali-catalyzed, acid-catalyzed, heterogeneous acid-catalyzed and supercritical processes, respectively. The vessels were specified to have an aspect ratio of 3-to-1.

2.4.2 Columns

Distillation column diameters were sized by two methods. An initial diameter was estimated from the F-Factor Method (Luyben 2002). If the column diameter was calculated to be greater than 0.90 m (2.95 feet) it was specified as a tray tower, and thus calculated from the flooding velocity using the Fair correlation (Seider et al. 2003). Columns with diameters calculated at less than 0.9 m were specified as a packed tower. The diameter of each packed column was calculated from the flooding velocity obtained from the Leva correlation (Seider et al. 2003).Tray tower height was calculated by multiplying the number of actual stages by the tray spacing, and then increasing the result by 20% to provide height for the condenser and reboiler. Packed tower height was calculated by multiplying the height equivalent of a theoretical plate (HETP) by the number of stages calculated for the tower. HETP was assumed to equal the column diameter (Seider et al. 2003). As for the height of a tray tower, the packed height was increased by 20%. The liquid-liquid extraction columns were sized according to the work of Zhang et al. (2003a).

2.4.3 Gravity separators

The gravity separators in the heterogeneous acid-catalyzed and supercritical processes were designed as vertical process vessels with an aspect ratio of 2. They were sized to allow for continuous operation, with a residence time of 1 hour.

2.4.4 Hydrocyclone

The initial dimensions of the hydrocyclone (used to separate the solid catalyst from the product stream in Process III) were calculated by the block in HYSYS. Those dimensions were then manipulated slightly to obtain complete removal of the catalyst in the hydrocyclone underflow.

2.5 Economic assessment

Since each process was capable of producing biodiesel at the required purity, it was of interest to conduct an economic assessment to determine process viability, and determine if any one process was advantageous over the others. As with the sizing calculations, all the economic calculations were performed within the HYSYS spreadsheet. Additionally, the values presented for the economic analysis are the values obtained after performing sensitivity analyses and optimization of each process. The details for the sensitivity analyses and optimization studies are presented in Section 2.6 of this paper. All parameters necessary to determine material and energy costs were imported to the spreadsheet from the flowsheet. Costing equations were incorporated directly into the spreadsheet as well. Individual unit costs were calculated, as well as figures for each process in its entirety. Incorporating the economic calculations into the simulation allowed for automatic recalculation of process economics should any process parameters, such as component flowrates or unit operating conditions be changed. By integrating sizing and economic calculations into each simulation, the potential to perform economic sensitivity analyses is automatically built-in to each simulation.

2.5.1 Basis of calculations

Each process was based on a plant capacity of 8000 tonnes/year biodiesel production. Operating hours were set at 7920 hours/year (assuming 330 operating days). Both the waste and pure feedstocks were assumed free of water and solid impurities, to avoid pre-treatment of the feed. Low and high pressure steam were used as heating media, while water was used for cooling. Each process was evaluated based on total capital investment (TCI), total manufacturing cost (TMC), and after tax rate-of-return (ATROR). The assessment performed in this work is classified as a "study estimate," with a range of expected accuracy from +30% to –20% (Turton et al. 2003). While the results of such a study will likely not reflect the final cost of constructing a chemical plant, the technique is useful for providing a relative means to compare competing processes.

2.5.2 Total capital investment

Table 2.8 gives a breakdown of the total capital investment. It also presents the costs for the individual unit operations in each process. Bare module capital costs (C_{BM}) consist of the purchase cost of a piece of equipment, multiplied by the bare module factor. Purchase costs were estimated for each piece of equipment based on a capacity equation presented by Turton et al. (2003)

$$\log_{10} C_p^\circ = K_1 + K_2 \log_{10}(A) + K_3 [\log_{10}(A)]^2 \tag{2.2}$$

where K_i is a constant specific to the unit type and A is the capacity of the unit. Bare module cost was calculated from

$$C_{BM} = C_p^\circ F_{BM} \tag{2.3}$$

where F_{BM} is given by

$$F_{BM} = (B_1 + B_2 F_M F_P) \tag{2.4}$$

where B_1 and B_2 are constants specific to the unit type, and F_M and F_P are the material and pressure factors, respectively. The constants, K_i and B_i, as well as the pressure and material factors were obtained from Turton et al. (2003) Equations 2.2 – 2.4 were encoded within the costing spreadsheet to allow for automatic cost updates when process parameters are changed.

2.5.3 Total manufacturing cost

Direct manufacturing expenses were calculated based on the price and consumption of each chemical and utility. Chemical and utility prices are presented in Table 2.9 and material flow information was obtained from HYSYS. Operator salary was estimated at $47,850/year, and it was assumed that an operator worked 49 weeks/year, and there were three 8-hour shifts per day for the continuous plant (Zhang et al. 2003b). Table 2.10 presents a breakdown of the components of the total manufacturing cost as well as the results for each process. After tax rate-of-return is a general criterion for economic performance of a chemical plant. It is defined as the percentage of net annual profit after taxes, relative to the total capital investment. Net annual profit after taxes (A_{NNP}) is half the net annual profit (A_{NP}) assuming a corporate tax rate of 50%. The results for after tax rate of return for each process are shown in Table 2.10.

As shown in Table 2.8, the transesterification reactor forms a large part of the capital cost, especially for Processes II and IV. The reactor in Process II was required to contain a large material flow at a long residence time. The presence of sulfuric acid as the catalyst required a

stainless steel reactor, resulting in a substantially higher reactor cost. Consequently the reactor in Process II was much more expensive than in all other processes. The supercritical reactor was required to withstand a high pressure, and was constructed from stainless steel to prevent oxidation and corrosion, hence its high cost. Distillation columns also contributed a significant part to the capital cost of each process. Tower costs for the methyl-ester purification tower were roughly equal between the processes, as each tower was handling approximately the same material flows and producing biodiesel at equal purities. The methanol recovery columns in Processes I and III were the least expensive, as they had the smallest material flow requirements. In spite of Process IV having the smallest number of unit operations, Process III had the smallest total capital investment. This is due to the fact that Process IV required a more expensive reactor in order to withstand the high pressures and corrosive conditions associated with the supercritical state of the alcohol, as well as the larger methanol recovery tower. The total capital investment for Process I in the present work was calculated to be $960 thousand, less than the value reported by Zhang et al. (2003b) of $1.34 million. The difference lies mostly in the lower costs calculated for the methanol recovery column and methyl-ester purification column, due to the differences in sizing.

Results for the total manufacturing cost of each process are shown in Table 2.10. The direct manufacturing cost represents between 71-77% of the total manufacturing cost in each process. The largest proportion of the direct manufacturing cost is due to the oil feedstock – up to 57% for Process I, and around 43% for the other processes. Process III has the lowest total manufacturing cost. This is due to both the ability of the process to use low cost waste vegetable oil, as well as the lower utility costs of the process resulting from the smaller material streams handled in the process. The total manufacturing cost of Process IV is slightly more than that of Process III, owing to the large energy requirements necessary to separate the methanol from the product stream.

Except for Process III, all processes had a negative after tax rate-of-return. Process I had the lowest ATROR, at −141%, while Processes II and IV had ATRORs at −4% and −0.9%, respectively. The ATROR for Process III was 54%, indicating that the process could earn a profit without any government subsidies. The value for ATROR reported by Zhang et al. (2003b) for Process I was −85% which is quite different from the value reported in this work. Comparing results, the utilities consumption, as well as the cost of waste disposal were much

higher in the present work, leading to a greater TMC. As well, the TCI was lower, and as its value decreases, the ATROR becomes larger in magnitude. However, our rate of return for process II (-4%) was in close agreement with the value reported for the acid-catalyzed case by al of −15%. Although the difference in magnitude between the ATROR calculated for Processes I and II is larger than that reported by Zhang et al. (2003b) the relative order of Processes I and II (i.e. that Process II has an ATROR greater than that of Process I) as presented in this work is in agreement with that of Zhang et al. (2003b). As predicted by Lotero et al. (2005), the heterogeneous acid-catalyzed process was by far the most economically attractive process.

2.6   Sensitivity analyses and optimization

Sensitivity analyses were conducted to determine the effect on the process of variables that had some degree of uncertainty; and to identify any operating specifications within an individual process that could be modified to improve the process.

Since the conversion data for the heterogeneous acid-catalyzed and supercritical processes were taken from bench-scale research, the economics of scale may not be accurately reflected. Thus the effect of reduced conversion on the overall process economics was examined for each process. As shown in Figure 5, conversion in the heterogeneous acid-catalyzed process must drop to approximately 85%, while conversion in the supercritical and homogeneous acid-catalyzed processes must increase to almost 100% before there is any overlap in the ATROR. From this, it is clear that even at reduced reactor conversion, the heterogeneous process will still be advantageous over the supercritical and homogeneous acid-catalyzed processes.

Sensitivity analyses were performed for all processes to determine the effect of changing methanol recovery in the methanol recovery distillation column on the ATROR. In all cases except the alkali-catalyzed case, increasing the methanol recovery caused an increase in the ATROR, due to decreased methanol consumption in all cases. Methanol acts as a cosolvent (Chiu et al. 2005) increasing the solubility of biodiesel in the glycerol phases. Therefore, reducing the amount of methanol entering the three phase separator (HAC and SC processes) reduced the amount of biodiesel lost in the glycerol stream, thereby boosting ATROR for both processes. Figure 2.6 illustrates the effect of methanol recovery on ATROR for the HAC process. Methanol recovery is limited to about 85%, as the bottoms stream temperature should not exceed 150°C. In order to increase the methanol recovery, the distillation column was

21

operated under vacuum conditions. The effect of vacuum pressure (and therefore cost of the vacuum system) on the ATROR was investigated to determine if the cost of the vacuum system was offset by the increase in revenue that results from higher methanol recovery. As shown in Figure 2.7, the addition of the vacuum system resulted in a decrease in ATROR. However, as the methanol recovery was increased under vacuum operation, the ATROR increased, indicating the potential for optimization of the column operating conditions to maximize the ATROR. Similar analyses were conducted for the homogeneous acid catalyzed and supercritical processes, but it was found that vacuum operation did not provide any economic benefits, as the methanol recovery was already greater than 99% and the bottoms temperature was within the allowable limit at ambient pressure operation. The HYSYS optimizer tool was used to vary the HAC methanol recovery in order to maximize the ATROR, according to the following constraints: bottoms temperature < 150°C; 1 kPa < column pressure < 100 kPa; and 85.0% < methanol recovery < 99.9%. An optimum was found at a pressure equal of 40 kPa and methanol recovery of 99.9%. Upon optimization the bottoms temperature decreased from 149.9°C to 145.5°C, methanol recovery increased from 85% to 99.9% and the ATROR increased slightly from 53.7% to 54.2%. In addition to the financial incentive, including a vacuum system reduces methanol consumption and eliminates 79200 kg/yr of methanol from the waste stream, greatly reducing the environmental impact of the process.

Lastly, the effect of vacuum operation in the fatty acid methyl-ester (FAME) distillation columns was investigated for the heterogeneous acid-catalyzed and the supercritical processes, to determine if vacuum operation would result in a net savings due to a decrease in the heating and cooling duties on the column. Column heating and cooling loads did decrease; however, the savings in utilities cost was not enough to offset the cost of the vacuum system, and inclusion of a vacuum system therefore decreased the ATROR in both cases. Since the upper temperature limit of biodiesel did not exceed at ambient operation a vacuum system was deemed unnecessary for FAME distillation in both processes. Vacuum operation for FAME distillation was needed in the homogeneous acid-catalyzed process to keep the temperature of the distillate below 250°C.

2.7   Conclusion

Four continuous processes to produce biodiesel at a rate of 8000 tonnes/year were designed and simulated in HYSYS. The processes were as follows: (I) a homogeneous alkali-catalyzed

process that used pure vegetable oil as the feedstock; (II) a homogeneous acid-catalyzed process that converted waste vegetable oil as the feedstock; (III) a heterogeneous acid-catalyzed process that used waste vegetable oil; and (IV) a supercritical non-catalyzed process, that consumed waste vegetable oil. From a technical standpoint, all processes are capable of producing biodiesel that meets ASTM specifications for purity. The supercritical process is the simplest and has the fewest number of unit operations, but requires severe operating conditions to achieve a high conversion of the feedstock. The heterogeneous acid-catalyzed process has one more unit than the supercritical process (a hydrocyclone to remove the solid catalyst) but operates at mild process conditions. The homogeneous processes had the greatest number of unit operations, and were more complicated, owing to the difficulty in removing the catalyst from the liquid phase.

An economic assessment revealed that the heterogeneous acid-catalyzed process has the lowest total capital investment, owing to the relatively small sizes and carbon steel construction of most of the process equipment. Raw materials consumed in the process account for a major portion of the total manufacturing cost. Accordingly, Processes II, III and IV have much lower manufacturing costs than Process I. The large excesses of methanol in Processes II and IV resulted in much higher utility costs than in process III making process III the only process to produce a net profit. The after tax rate of return for Process III was 54%, while Processes I, II and IV had rates of return of –144%, –4% and –0.9%, respectively.

Sensitivity analyses were conducted to identify any unit operations were operating specifications could be modified to improve the process. Increasing methanol recovery led to a greater ATROR. Accordingly, methanol recovery was set as high as possible (>99%) before the glycerol degradation temperature (150°C) was exceeded in the homogeneous acid-catalyzed and supercritical processes. Use of the optimizer function indicated a vacuum system could be installed in the heterogeneous acid-catalyzed (HAC) process to increase methanol recovery and consequently the ATROR, while keeping the bottoms stream within the temperature limit.

An analysis of the effect of reaction conversion on ATROR revealed that even at reduced reaction conversion (i.e., between 85-93%) , the ATROR of the HAC process is greater than at 100% conversion of the homogeneous acid and supercritical processes.

23

Therefore Process III, the heterogeneous acid-catalyzed process, is clearly advantageous over the other processes, as it had the highest rate of return, lowest capital investment, and technically, was a relatively simple process. Further research in developing the heterogeneous acid-catalyzed process for biodiesel production is warranted.

Table 2.1. Catalysts and reaction parameters for heterogeneously catalyzed reactions of soybean oil at 1 atm.

	Reaction Parameters			
Catalyst type	A:O Molar ratio	Temperature	Conversion	Time
WO_3/ZrO_2 (Furuta et al. 2004)	40:1	>250 °C	>90%	4 h
SO_4/SnO_2 (Furuta et al. 2004)	40:1	300°C	65%	4 h
SO_4/ZrO_2 (Furuta et al. 2004)	40:1	300°C	80%	4 h
SnO (Abreu et al. 2005)	4.15:1	60°C	94.7	3 h

Table 2.2. Summary of unit operating conditions for each process.

		Alkali-Catalyzed (Process I)	Acid-Catalyzed (Process II)	Heterogeneous Acid-Catalyzed (Process III)	Supercritical Process (Process IV)
Transesterification					
	Catalyst	NaOH	H_2SO_4	SnO	N/A
	Reactor Type	CSTR	CSTR	Multiphase	CSTR
	Temperature (°C)	60	80	60	350
	Pressure (kPa)	400	400	101.3	20×10^3
	A:O Ratio	6:1	50:1	4.5:1	42:1
	Residence time (hr)	4	4	3	0.333
	Conversion (%)	95	97	94	98
Methanol Recovery					
	Reflux Ratio	2	2	3.99	3.42
	Number of stages	6	6	14	12
	Condenser/Reboiler Pressure (kPa)	20/30	101.3/111	40/50	101.3/105.3
	%Recovery	94	99.2	99.9	99.3
	Distillate flowrate (kg/h)	113.14	1687	66.33	1239.7
	Distillate purity(%)	100	100	99.9	99.99
Catalyst Removal		N/A[a]	N/A[a]	hydrocyclone	N/A
Glycerine Separation		Water washing	Water washing	Gravity separation	Gravity separation
	Water flowrate	11 kg/h	46 kg/h	–	–
Catalyst Neutralization					
	Neutralizing agent	H_3PO_4	$CaSO_4$	N/A	N/A
Biodiesel Purification					
	Reflux ratio	1.85	2	2	2
	Number of stages	6	10	8	8
	Condenser/reboiler Pressure (kPa)	10/20	10/15	101.3/111.3	101.3/111.3
	%Recovery	99.9	98.65	99.9	99.9
	Final purity	99.9	99.65	99.9	99.65

Table 2.3. Feed and product stream information for the alkali-catalyzed process.

	Feed Streams				Product Streams				
	101	105-PVO	103		401A	401	402	501	502
Temperature (°C)	25.0	25.0	25.0	Temperature (°C)	167.8	167.5	463.9	42.8	148.6
Pressure (kPa)	101.3	101.3	101.3	Pressure (kPa)	10	10	15	20	30
Molar flow (kgmol/h)	3.61	1.19	0.25	Molar flow (kgmol/h)	0.12	3.38	0.06	0.65	1.20
Mass flow (kg/h)	115.71	1050.00	10.00	Mass flow (kg/h)	4.57	1001.8	52.77	13.79	105.12
Component mass fraction				Component mass fraction					
Methanol	1.000	0.000	0.000	Methanol	0.6114	0.0001	0.0000	0.3432	0.0001
Triolein	0.000	1.000	0.000	Glycerol	0.0005	0.0000	0.0000	0.0002	0.9865
NaOH	0.000	0.000	1.000	Triolein	0.0000	0.0001	0.9967	0.0000	0.0014
				M-oleate	0.2125	0.9997	0.0033	0.0000	0.0002
				NaOH	0.0000	0.0000	0.0000	0.0000	0.0000
				H3PO4	0.0000	0.0000	0.0000	0.0000	0.0000
				Na3PO4	0.0000	0.0000	0.0000	0.0000	0.0000
				Water	0.1755	0.0000	0.0000	0.6565	0.0119

Table 2.4. Feed and product stream information for the homogeneous acid-catalyzed process.

	Feed Streams				Product Streams				
	101	103	105		401A	401	402	501	502
Temperature (°C)	25	25	25	Temperature (°C)	130.7	234.3	502.2	23.4	226.6
Pressure (kPa)	101.3	101.3	101.3	Pressure (kPa)	35	45	55	10	15
Molar flow (kgmol/h)	3.78	1.53	1.17	Molar flow (kgmol/h)	0.65	3.42	0.05	6.59	1.10
Mass flow (kg/h)	121.2	150.06	1030.00	Mass flow (kg/h)	20.42	1002.98	33.22	155.64	101.69
Component mass fraction				Component mass fraction					
Methanol	1.000	0.000	0.000	Methanol	0.957	0.001	0.000	0.520	0.000
Triolein	0.000	0.000	0.950	Glycerol	0.001	0.000	0.000	0.009	0.993
H_2SO_4	0.000	1.000	0.000	Triolein	0.000	0.001	0.889	0.000	0.007
Oleic Acid	0.000	0.000	0.050	H2SO4	0.000	0.000	0.000	0.000	0.000
				M-oleate	0.007	0.998	0.111	0.003	0.000
				CaO	0.000	0.000	0.000	0.000	0.000
				Water	0.035	0.000	0.000	0.468	0.000
				Oleic Acid	0.000	0.000	0.000	0.000	0.000

Table 2.5. Feed and product stream information for the heterogeneous acid-catalyzed process.

	Feed Streams				Product Streams		
	Methanol 101	SnO 103	Triolein 105		302 Glycerol Out	401	402
Temperature (°C)	25.0	25.0	25.0	Temperature (°C)	25.0	203.2	535.5
Pressure (kPa)	101.3	101.3	101.3	Pressure (kPa)	50	101.3	111.3
Molar flow (kgmol/h)	3.38	0.04	1.31	Molar flow (kgmol/h)	1.22	3.38	0.07
Mass flow (kg/h)	108.3	10.54	1050.00	Mass flow (kg/h)	100.4	989.6	59.80
Component mass fraction				Component mass fraction			
Methanol	1.0000	0.0000	0.0000	Methanol	0.0004	0.0000	0.0000
Triolein	0.0000	0.0000	0.9500	glycerol	0.9625	0.0001	0.0001
Tin(II) oxide	0.0000	1.0000	0.0000	triolein	0.0064	0.0000	0.9835
Oleic acid	0.0000	0.0000	0.0500	M-oleate	0.0002	0.9995	0.0165
				tin(II) oxide	0.0000	0.0000	0.0000
				Oleic acid	0.0000	0.0000	0.0000
				water	0.0304	0.0002	0.0000

Table 2.6. Feed and product stream information for the supercritical methanol process.

	Feed Streams			Product Streams		
	101 Methanol	103 Triolein		302 Glycerol Out	401	402
Temperature (°C)	25	25	Temperature (°C)	25	134.5	463.7
Pressure (kPa)	100	100	Pressure (kPa)	105.3	101.3	111.3
Molar flow (kgmol/h)	3.67	1.31	Molar flow (kgmol/h)	1.44	3.62	0.03
Mass flow (kg/h)	117.8	1050.00	Mass flow (kg/h)	110.1	1039.4	20.83
Component mass fraction			Component mass fraction			
Methanol	1.0000	0.0000	Methanol	0.0501	0.0030	0.0000
Triolein	0.0000	0.9500	Glycerol	0.9180	0.0006	0.0000
Oleic acid	0.0000	0.0500	Triolein	0.0012	0.0000	0.9947
			M-oleate	0.0033	0.9960	0.0052
			Oleic acid	0.0000	0.0000	0.0000
			water	0.0272	0.0003	0.0000

Table 2.7. Equipment sizes for various process units in all processes. (Dimensions are diameter x height, m).

Type	Description	Alkali-Catalyzed (Process I)	Acid-Catalyzed (Process II)	Heterogeneous Acid-Catalyzed (Process III)	Supercritical Process (Process IV)
Reactor					
	Transesterification	1.8x5.4	2.1x6.3	1.2x3.64	0.96x2.9
	Neutralization	0.36x1.1	0.5x1.5	N/A	N/A
Columns					
	Methanol Recovery	0.46x3	0.9x8.6	0.31x7.4	1x8.8
	Fame Purification	0.9x9.5	1x8.5	0.9x6.6	1x6.6
	Water Washing	0.8x10	1x10	N/A	N/A
	Glycerol Purification	N/A	0.5x3.7	N/A	N/A
Separators					
	Gravity Separators	N/A	N/A	1.2x2.4	1.1x2.4
	Hydrocyclone	N/A	N/A	0.112x1.35	N/A

Table 2.8. Equipment costs, fixed capital costs and total capital investments for each process. (Units: $millions).

Type	Description	Alkali-Catalyzed	Acid-Catalyzed	Solid Acid-Catalyzed	Supercritical Process
Reactor					
	Transesterification	0.292	0.680	0.075	0.639
	Neutralization	0.027	0.036	0	0
Columns					
	Methanol Recovery	0.038	0.152	0.028	0.167
	Fame Purification	0.102	0.076	0.095	0.146
	Washing	0.084	0.113	0	0
	Glycerol Purification	0	0.028	0	0
Other					
	Gravity Separators	0	0	0.057	0.058
	Heat Exchangers	0	0.079	0.079	0.109
	Pumps	0.014	0.010	0.014	0.141
	Others (hydrocyclone etc)	0	0	0.015	0
Total bare module cost, C_{BM}		0.56	1.17	0.37	1.26
Contingency fee, $C_{CF} = 0.18 C_{BM}$		0.10	0.22	0.07	0.23
Total module cost, $C_{TM} = C_{BM} + C_{CF}$		0.67	1.38	0.43	1.49
Auxiliary facility cost, $C_{AC} = 0.3 C_{BM}$		0.17	0.35	0.11	0.38
Fixed Capital Cost, $C_{FC} = C_{TM} + C_{AC}$		0.83	1.73	0.54	1.87
Working capital $C_{WC} = 0.15 C_{FC}$		0.13	0.26	0.08	0.28
Total capital investment $C_{TCI} = C_{FC} + C_{WC}$		0.95	1.99	0.63	2.15

Table 2.9. Conditions for the economic assessment of each process. (Zhang et al. 2003b)

Item	Specification	Price ($/tonne)
Chemicals		
Biodiesel		600
Calcium Oxide		40
Glycerine	92 wt.%	1200
	85 wt.%	750
Methanol	99.85%	180
Phosphoric Acid		340
Sodium Hydroxide		4000
Sulfuric Acid		60
Tin (II) Oxide		600
Pure canola oil		500
Waste cooking oil		200
Utilities		
Cooling water	400 kPa 6 °C	$0.007/m^3
Electricity		$0.062/kWh
Low pressure steam[a]	601.3 kPa 160°C	$7.78/GJ
High pressure steam[a]	4201.3 kPa 254°C	$19.66/GJ

[a] Value from[(Turton et al. 2003)]

Table 2.10. Total manufacturing cost and after tax rate-of-return for each process. (Units: $millions).

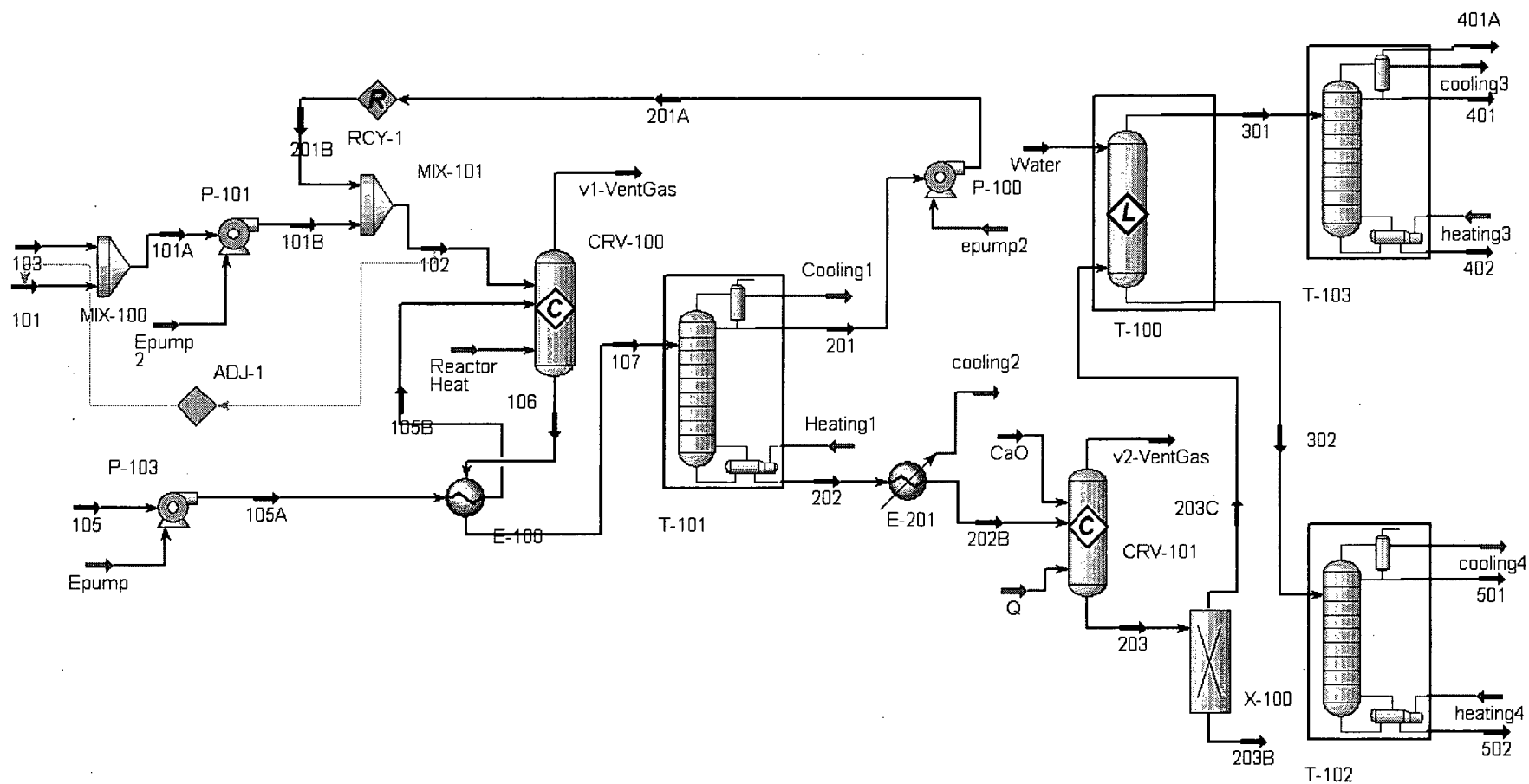|	Process I	Process II	Process III	Process IV
Direct manufacturing cost				
Oil feedstock	4.16	1.63	1.66	1.66
Methanol	0.16	0.30	0.16	0.17
Catalyst	0.34	0.10	0.05	0.00
Operating Labour	0.58	0.58	0.58	0.58
Supervisory Labour	0.09	0.09	0.09	0.09
LP steam	0.03	0.36	0.05	0.39
HP steam	0.26	0.25	0.28	0.33
Electricity	0.00	0.00	0.00	0.00
Cooling Water	0.01	0.02	0.01	0.02
Liquid waste disposal	0.07	0.09	0.05	0.02
Solid waste disposal	0.01	0.06	0.02	0.00
Maintenance and Repairs (M&R), 6% of C_{FC}	0.05	0.11	0.03	0.11
Operating Supplies, 15% of M&R	0.01	0.02	0.00	0.02
Lab charges, 15% of operating labour	0.09	0.09	0.09	0.09
Patents and royalties, 3% TMC	0.22	0.15	0.12	0.14
Subtotal A_{DMC}	6.07	3.84	3.19	3.61
Indirect manufacturing cost				
Overhead, packaging and storage,				
60% of sum of operating labour , supervision				
and maintenance	0.43	0.46	0.42	0.47
Local Taxes, 1.5% of C_{FC}	0.01	0.03	0.01	0.03
Insurance, 0.5% of C_{FC}	0.00	0.01	0.00	0.01
Subtotal, A_{IMC}	0.43	0.47	0.42	0.47
Depreciation 10% of C_{FC}	0.08	0.18	0.05	0.19
General expenses				
Administrative costs, 25% of overhead	0.11	0.12	0.10	0.12
Distribution and selling, 10% of TMC	0.73	0.48	0.39	0.46
Research &Development, 5% of TMC	0.36	0.24	0.19	0.23
Subtotal	1.20	0.84	0.69	0.81
Total production cost	7.89	5.44	4.45	5.19
Glycerine Credit	0.62	0.60	0.57	0.60
Total Manufacturing Cost, A_{TE}	7.28	4.83	3.88	4.59
Revenue from Biodiesel	4.75	4.76	4.70	4.92
Net annual profit	-2.53	-0.08	0.82	0.33
Income taxes, A_{IT} 50% of A_{NP}	-1.26	-0.04	0.41	0.17
Net annual after tax profit, A_{NNP}	-1.26	-0.04	0.41	0.17
After tax rate of return, I = $[A_{NNP}-A_{BD}]/C_{TC}$	-141.74%	-10.61%	58.76%	-0.90%

Figure 2.1. Alkali-catalyzed process flowsheet (Process I).

Figure 2.2. Homogeneous acid—catalyzed process flowsheet (Process II)

Figure 2.3. Heterogeneous acid—catalyzed process flowsheet (Process III).

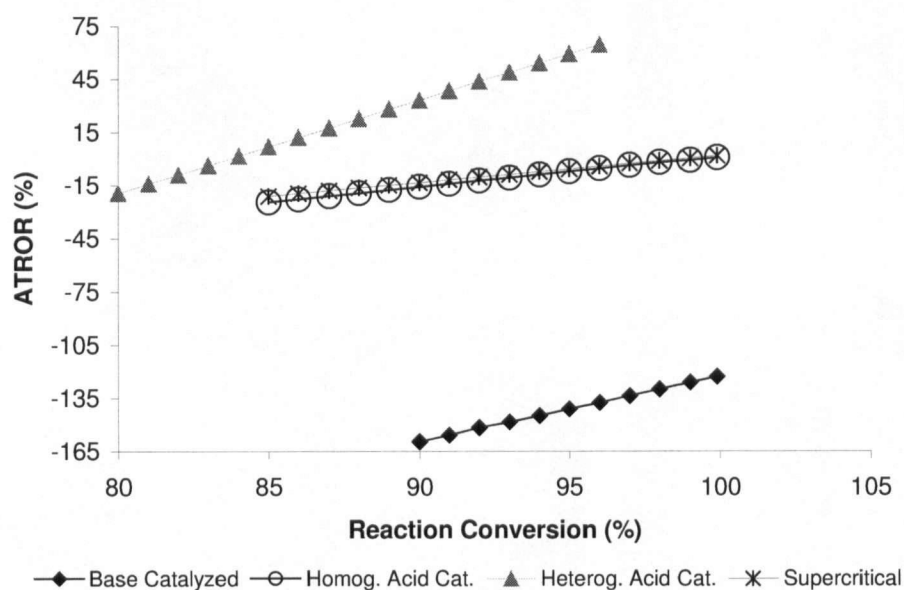**Figure 2.4**. Supercritical alcohol process flowsheet (Process IV).

Figure 2.5. After-tax rate of return vs. reaction conversion for all processes.
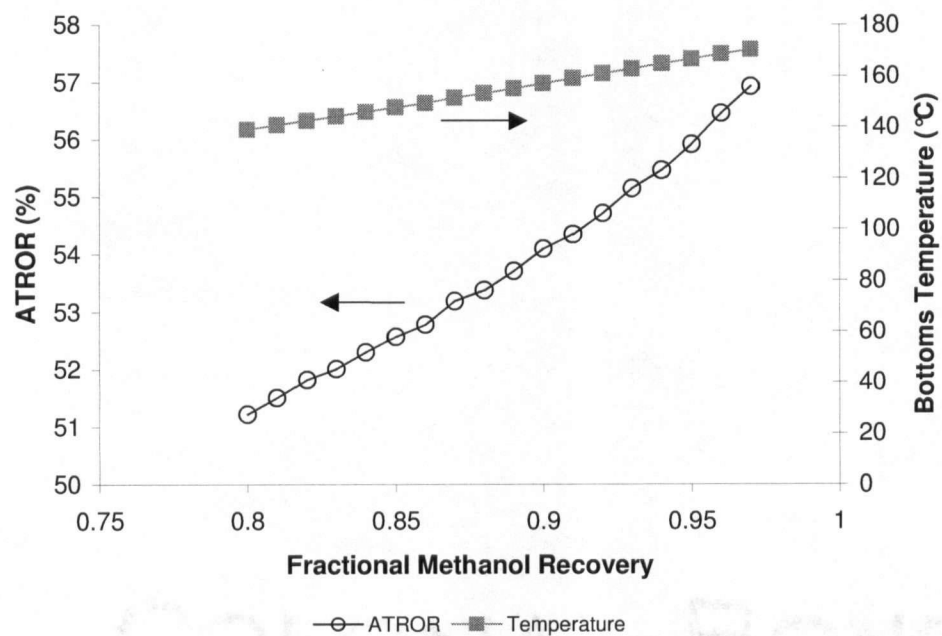
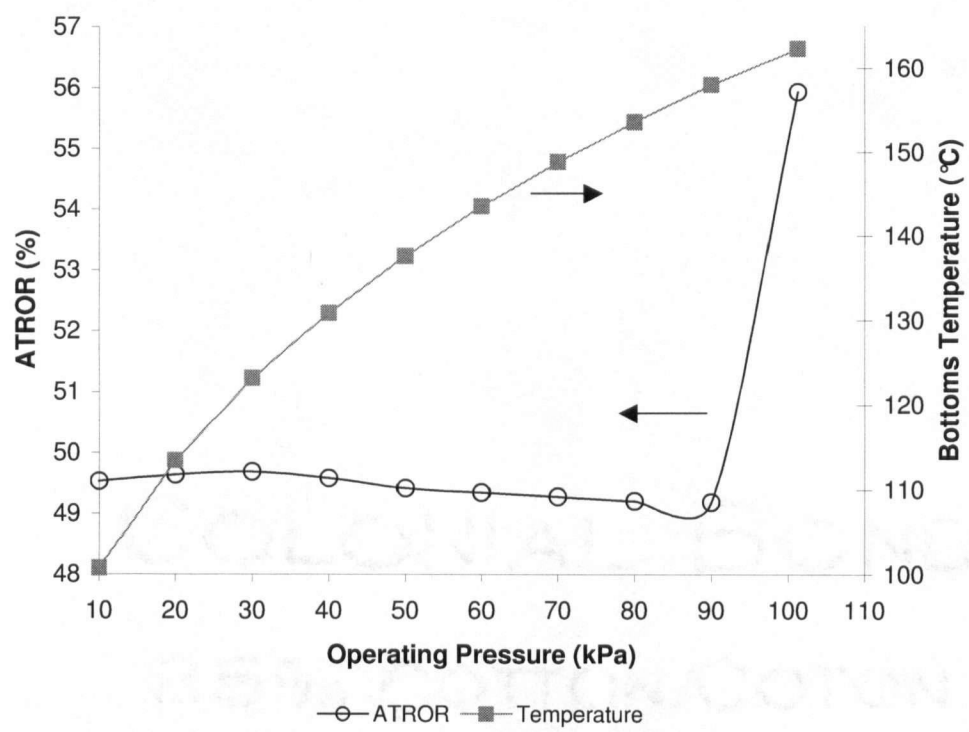**Figure 2.6.** ATROR vs. methanol recovery in the methanol recovery column, HAC process.

Figure 2.7. ATROR vs. operating pressure in the methanol recovery column, HAC process.

References

Abreu, F. R., Alves, M. B., Macedo, C. C. S., Zara, L. F. and Suarez, P. A. Z. (2005). New multi-phase catalytic systems based on tin compounds active for vegetable oil transesterification reaction. Journal of Molecular Catalysis A: Chemical 227(1-2): 263-267.

Canakci, M. and Van Gerpen, J. (1999). Biodiesel production via acid catalysis. Transactions of the ASAE 42(5): 1203-1210.

Canakci, M. and Van Gerpen, J. (2001). Biodiesel production from oils and fats with high free fatty acids. Transactions of the ASAE 44(6): 1429-1436.

Canakci, M. and Van Gerpen, J. (2003). A pilot plant to produce biodiesel from high free fatty acid feedstocks. Transactions of the ASAE 46(4): 945-954.

Chiu, C. W., Goff, M. J. and Suppes, G. J. (2005). Distribution of methanol and catalysts between biodiesel and glycerin phases. AICHE Journal 51(4): 1274-1278.

Delfort, B., Hillion, G., Le Pennec, D., Chodorge, J. A. and Bournay, L. (2003). Biodiesel production by a continuous process using a heterogeneous catalyst. Abstracts of Papers of the American Chemical Society 226: U539-U539.

Demirbas, A. (2002). Biodiesel from vegetable oils via transesterification in supercritical methanol. Energy Conversion and Management 43(17): 2349-2356.

Freedman, B., Butterfield, R. O. and Pryde, E. H. (1986). Transesterification kinetics of soybean oil. Journal of the American Oil Chemists Society 63(10): 1375-1380.

Freedman, B., Pryde, E. H. and Mounts, T. L. (1984). Variables affecting the yields of fatty esters from transesterified vegetable-oils. Journal of the American Oil Chemists Society 61(10): 1638-1643.

Furuta, S., Matsuhashi, H. and Arata, K. (2004). Biodiesel fuel production with solid superacid catalysis in fixed bed reactor under atmospheric pressure. Catalysis Communications 5(12): 721-723.

Goff, M. J., Bauer, N. S., Lopes, S., Sutterlin, W. R. and Suppes, G. J. (2004). Acid-catalyzed alcoholysis of soybean oil. Journal of the American Oil Chemists Society 81(4): 415-420.

Goodrum, J. W. (2002). Volatility and boiling points of biodiesel from vegetable oils and tallow. Biomass & Bioenergy 22(3): 205-211.

Haas, M. J., McAloon, A. J., Yee, W. C. and Foglia, T. A. (2006). A process model to estimate biodiesel production costs. Bioresource Technology 97(4): 671-678.

Krawczyk, T. (1996). Biodiesel. INFORM 7(8): 801-822.

Kusdiana, D. and Saka, S. (2001). Kinetics of transesterification in rapeseed oil to biodiesel fuel as treated in supercritical methanol. Fuel 80(5): 693-698.

Kusdiana, D. and Saka, S. (2004). Effects of water on biodiesel fuel production by supercritical methanol treatment. Bioresource Technology 91(3): 289-295.

Lotero, E., Liu, Y. J., Lopez, D. E., Suwannakarn, K., Bruce, D. A. and Goodwin, J. G. (2005). Synthesis of biodiesel via acid catalysis. Industrial & Engineering Chemistry Research 44(14): 5353-5363.

Luyben, W. L. (2002). Plantwide dynamic simulators in chemical processing and control. New York, Marcel Dekker.

Ma, F. R. and Hanna, M. A. (1999). Biodiesel production: A review. Bioresource Technology 70(1): 1-15.

McCabe, W. J., Smith, J. C. and Harriott, P. (2001). Unit operations of chemical engineering. 6th ed.

Newman, A. A. (1968). Glycerol. Cleveland, CRC Press.

Saka, S. and Kusdiana, D. (2001). Biodiesel fuel from rapeseed oil as prepared in supercritical methanol. Fuel 80(2): 225-231.

Schumacher, L. G., Marshall, W., Krahl, J., Wetherell, W. B. and Grabowski, M. S. (2001). Biodiesel emissions data from series 60 ddc engines. Transactions of the ASAE 44(6): 1465-1468.

Seider, W. D., Seader, D. and Lewin, D. R. (2003). Process design principles: Synthesis, analysis and evaluation. Chichester, UK, John Wiley & Sons.

Suppes, G. J., Dasari, M. A., Doskocil, E. J., Mankidy, P. J. and Goff, M. J. (2004). Transesterification of soybean oil with zeolite and metal catalysts. Applied Catalysis a-General 257(2): 213-223.

Turton, R., Bailie, R. C., Whiting, W. B. and Shaeiwitz, J. A. (2003). Analysis, synthesis, and design of chemical processes. Upper Saddle River, New Jersey, Prentice Hall.

Tyson, K. S. Biodiesel: Handling and use guidelines. http://www.eere.energy.gov/biomass/pdfs/biodiesel_handling.pdf (November 28, 2004),

Warabi, Y., Kusdiana, D. and Saka, S. (2004). Reactivity of triglycerides and fatty acids of rapeseed oil in supercritical alcohols. Bioresource Technology 91(3): 283-287.

Zhang, Y., Dube, M. A., McLean, D. D. and Kates, M. (2003a). Biodiesel production from waste cooking oil: 1. Process design and technological assessment. Bioresource Technology 89(1): 1-16.

Zhang, Y., Dube, M. A., McLean, D. D. and Kates, M. (2003b). Biodiesel production from waste cooking oil: 2. Economic assessment and sensitivity analysis. Bioresource Technology 90(3): 229-240.

3 Characterization and Testing of Heterogeneous Catalysts for Biodiesel Production[2]
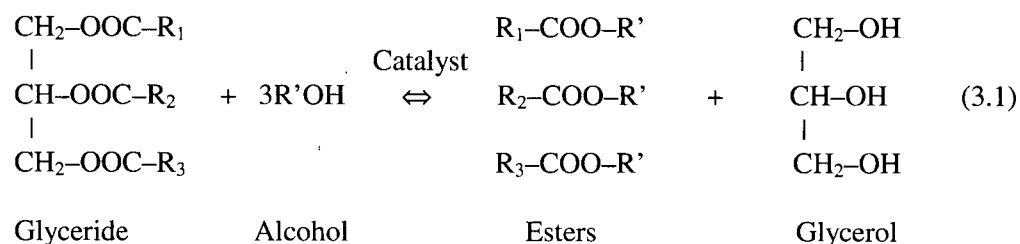
3.1 Introduction and background

Rising crude oil prices, concerns over diminishing fossil fuel reserves and regard for environmental quality, especially in urban areas, have all contributed to the large research efforts aimed at achieving economical means of producing alternative fuels derived from renewable resources, such as biodiesel and bioethanol.
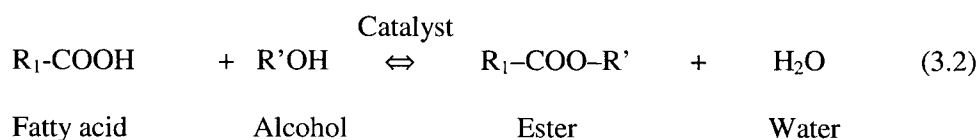
Biodiesel (mono-alkyl esters of long chain fatty acids) is a promising alternative (or extender) to conventional petroleum based diesel fuel. Biodiesel has a number of advantages when compared with regular diesel fuel. The first and foremost is that it is derived from a renewable domestic resource (vegetable oil), and has been shown to reduce carbon dioxide emissions by 78% (Tyson 2001) when compared to diesel fuel on a life cycle basis. Combustion of biodiesel has the potential to significantly lower greenhouse gas (GHG) emissions. For example, a 5 % biodiesel blend (B5) instituted nation-wide in Canada would reduce the amount of CO_2 entering the atmosphere by 2.5 MT (Holbein et al. 2004). Biodiesel contains no sulfur (and therefore emits no SO_x which is a precursor for acid rain), but provides greater lubricity than conventional diesel fuel, and can therefore enhance engine longevity. Lastly, biodiesel is non-toxic and biodegrable making it a more environmentally benign fuel.

Biodiesel is produced from the reaction of a vegetable oil or animal fat (which are composed of complex mixtures of triglycerides and free fatty acids depending on the quality of the oil or tallow) and a low molecular weight alcohol, such as methanol, ethanol or propanol. Methanol is most frequently used as it is the least expensive alcohol. The reaction between the triglyceride and the alcohol in the presence of a catalyst, depicted in Equation 3.1, is referred to as transesterification. The reaction produces a complex mixture of fatty acid methyl esters (the biodiesel product, which is dependant on the vegetable oil type), and glycerol.

---

[2] A version of this chapter is in preparation for submission for publication. West, A. H. and Ellis, N. (2006)

$$
\begin{array}{lllll}
\text{CH}_2\text{--OOC--R}_1 & & \text{R}_1\text{--COO--R'} & & \text{CH}_2\text{--OH} \\
| & \text{Catalyst} & & & | \\
\text{CH--OOC--R}_2 & +\ 3\text{R'OH} \quad \Leftrightarrow & \text{R}_2\text{--COO--R'} & + & \text{CH--OH} \qquad (3.1) \\
| & & & & | \\
\text{CH}_2\text{--OOC--R}_3 & & \text{R}_3\text{--COO--R'} & & \text{CH}_2\text{--OH}
\end{array}
$$

| Glyceride | Alcohol | Esters | Glycerol |

Biodiesel can also be produced through the reaction of free fatty acids (FFA) and alcohol in the presence of a catalyst to produce biodiesel and water (Equation 3.2).

$$
\begin{array}{lllll}
 & & \text{Catalyst} & & \\
\text{R}_1\text{-COOH} & +\ \text{R'OH} & \Leftrightarrow & \text{R}_1\text{--COO--R'} & + & \text{H}_2\text{O} \qquad (3.2)
\end{array}
$$

| Fatty acid | Alcohol | Ester | Water |

This reaction becomes significant in the case where the feedstock contains high amounts of FFA which can limit the yield of the process of the Transesterification, as water can deactivate the catalyst and lead to soap formation.

The transesterification reaction can be catalyzed through a number of different methods: homoegeneous alkali (Freedman et al. 1984); homogeneous acid (Canakci and Van Gerpen 1999); supercritical alcohol with no catalyst (Saka and Kusdiana 2001); and via heterogeneous catalysts. The homogeneous alkali-catalyzed method is the most well known and common industrial method. It provides high yields in short times at mild process conditions, but is the most expensive of the processes (Zhang et al. 2003), since it requires a pure vegetable oil feed (which can account for up to 75% of the cost of the process (Krawczyk 1996), as the base catalyzed process is highly intolerant of water and FFA in the feedstock (Freedman et al. 1984)). Homogeneous acid-catalyzed transesterification improves on the alkali-catalyzed method as it can accommodate lower quality (and therefore less expensive) feedstocks with FFA amounts up to 5 wt.%. However, at mild conditions, the process is extremely slow, and requires up to 48 hours to achieve conversions greater than 95%. It also requires a large excess of methanol. Although the process is more economical than the alkali-catalyzed method (Zhang et al. 2003), it is still disadvantageous. Furthermore, both processes require water to separate the catalyst from the product stream and a catalyst neutralization step, increasing the waste output and necessitating a more complicated process. The supercritical process eliminates the need for a

catalyst and gives very high yields in very short times (Warabi et al. 2004). However, these advantages are offset by the high cost of the equipment required to withstand such high pressures (West et al. 2006). Heterogeneous catalysis, in particular acid catalysis, presents a number of advantages suggesting the most economical process for biodiesel production (Lotero et al. 2005). Heterogeneous catalysts can be easily separated from the reaction mixture without the use of water, do not require neutralization and can therefore be potentially reused. In addition, acid catalysts show the potential to catalyze both esterification and transesterification (Furuta et al. 2004) reactions simultaneously, allowing lower cost feedstocks to be processed. A recent process simulation conducted by West et al. (2006) indicated the heterogeneous process to be the most economical compared with the supercritical and traditional homogeneous processes.

To this end, a number of researchers have investigated solid-acid catalysts, such as superacids, (Furuta et al. 2004; Lotero et al. 2005; Jitputti et al. 2006; Kiss et al. 2006) and as well as zeolytes and metal oxides (Lotero et al. 2005; Kiss et al. 2006). Although the range of temperatures, pressures and feestocks studied varied significantly, overall results were positive, with most catalysts achieving > 90% conversion. Recent research has also focused on designing catalysts to effectively catalyze the esterification of FFAs. Mbaraka and Shanks (2005) designed a mesoporous silica catalyst (MCM-41) with specially tailored hydrophobic groups to prevent catalyst deactivation by the water produced during the esterification reaction. Toda et al. (2005) prepared a heterogeneous acid catalyst from pyrolized sugar reacted with sulfuric acid and demonstrated its ability to esterify free fatty acids, although they did not report the yield of the process.

Research concerning heterogeneous catalysts for transesterification is still in the catalyst screening stage. Studies regarding reaction kinetics are few (Lopez et al. 2005), and studies aimed at improving reaction parameters have yet to be conducted. In addition, studies to determine the effects of free fatty acid concentration and water on the performance of the catalyst have been scarce. Based on the positive indication that the heterogeneous process was economical, SnO was selected for catalytic experiments to investigate the factors affecting SnO catalyzed transesterification (such as A:O molar ratio, FFA content, etc.). Another group of experiments was performed with an acid catalyst derived from pyrolysis char (sulfonated char),

to test its ability to catalyze both the transesterification and esterification reactions. Fast pyrolysis processes (heating of biomass in the absence of oxygen at rapid heating rates) generally have char yields between 10-25% by weight of the feedstock (Bridgwater et al. 1999; Dynamotiv 2006). The char can either be upgraded to activated carbon or used as an energy source, as it has a heating value comparable to lignite coal. The potential for upgrading a low-value product presents an attractive prospect, and therefore sulfonated char was investigated as a catalyst in biodiesel production.

3.2 Tin(II) oxide synthesis and testing methods

3.2.1 SnO synthesis procedure

Initial attempts at synthesizing SnO followed the method of (Abreu et al. 2005). Equimolar mixtures (2 mmol) of $SnCl_2$ dissolved in water (20 mL) and acetylacetone were mixed under basic conditions (2 mmol NaOH in the solution) and stirred with a magnetic stirrer at 40°C for 30 minutes on a hotplate (Barnstead Thermolyne Cimarec, Fisher Scientific). The mixture was then placed in a refrigerator overnight. The precipitate was isolated via vacuum filtration (Whatman #40 filter paper), dried in a dessicator overnight and then calcined at 500°C for 24 hours in air. A second method of SnO preparation followed that of Fujita et al. (1990): an acidic solution (pH 1.1, 100 mL) of hydrocholic acid and water containing 0.02 mol/L $SnCl_2$ and 0.6 mol/L urea was heated at 95-97°C under reflux on a hotplate under magnetic stirring for 1 hour, at which point a dark precipitate was observed to form. The precipitate was then isolated by vacuum filtration (Whatman #40) and washed with distilled water, before being dried at room temperature in a desiccator.

3.2.2 Catalyst testing

Both the prepared and commercial samples of SnO were tested as catalysts under similar conditions to the work of Abreu et al. (2005), in simple batch experiments. Reactions were carried out on a hotplate with magnetic stirring under reflux at 60°C, to determine the effect of A:O (methanol to canola oil respectively) molar ratio and reaction time on the conversion of the reaction. Reaction products were analyzed by GC, using a Hewlett-Packard 5890 with a flame ionization detector and a DB –5 capillary column (15 m 0.32 mm ID) (Agilent Technologies). The temperature program was as follows: Initial temperature of 45°C was held for 1 minute, and then heated at a ramp rate of 5°C/min to 300°C and held for 15 minutes. The injector and

detector temperatures were 290°C and 310°C, respectively, with no derivitization of the samples.

3.3 Tin(II) oxide results and discussion

3.3.1 Synthesis and characterization

The first procedure as noted in Abreu et al. (2005) to synthesize SnO did not result in any significant yield. The post-calcination product was an unknown substance, dull grey-beige in colour, in contrast to the shiny blue-black colour of a commercial sample of SnO as depicted in Figures 3.1 and 3.2, respectively. A subsequent review of the literature revealed that $SnCl_2$ will precipitate as SnOH under basic conditions (Fujita et al. 1990). Thus it was likely that the calcined product was some form of SnOH. Next, the method of Fujita et al. (1990) was adopted to successfully prepare SnO as confirmed by comparison of x-ray diffraction patterns of the prepared sample with the literature (Fujita et al. 1990), and with the pattern of a commercial sample shown in Figures 3.3 and 3.4, respectively.

3.3.2 Catalytic activity

Initial attempts to produce biodiesel by reacting canola oil and methanol (6:1 A:O molar ratio, 60°C, 5 wt.% catalyst under magnetic stirring and reflux) for 3 hours in the presence of the synthesized SnO sample proved unsuccessful. Subsequent attempts held the catalyst loading constant, and increased the A:O molar ratio (9:1, 15:1) and reaction times (12 hours, 24 hours) but no conversion was observed. The reaction mixture was analyzed by GC upon completing the reactions, and showed no methyl ester peaks when compared to a chromatograph from a pure biodiesel sample. Furthermore, no noticeable reaction had occurred when the commercial sample of SnO was used under reaction conditions identical to those described above. With no other material in the literature or correspondence with the authors Abreu et al. (2005) to support the activity of SnO in transesterification reaction, further attempts to produce biodiesel with SnO as the catalyst ceased.

3.4 Sulfonated char synthesis and testing mthods

3.4.1 Sulfonated char synthesis procedure

Pyrolyzed hardwood char samples were obtained from Resource Transforms International Ltd. (Waterloo ON.), Ensyn Technologies Inc. (Ottawa, ON) and Dynamotiv Energy Systems Corp.

detector temperatures were 290°C and 310°C, respectively, with no derivitization of the samples.

3.3 Tin(II) oxide results and discussion

3.3.1 Synthesis and characterization

The first procedure as noted in Abreu et al. (2005) to synthesize SnO did not result in any significant yield. The post-calcination product was an unknown substance, dull grey-beige in colour, in contrast to the shiny blue-black colour of a commercial sample of SnO as depicted in Figures 3.1 and 3.2, respectively. A subsequent review of the literature revealed that $SnCl_2$ will precipitate as SnOH under basic conditions (Fujita et al. 1990). Thus it was likely that the calcined product was some form of SnOH. Next, the method of Fujita et al. (1990) was adopted to successfully prepare SnO as confirmed by comparison of x-ray diffraction patterns of the prepared sample with the literature (Fujita et al. 1990), and with the pattern of a commercial sample shown in Figures 3.3 and 3.4, respectively.

3.3.2 Catalytic activity

Initial attempts to produce biodiesel by reacting canola oil and methanol (6:1 A:O molar ratio, 60°C, 5 wt.% catalyst under magnetic stirring and reflux) for 3 hours in the presence of the synthesized SnO sample proved unsuccessful. Subsequent attempts held the catalyst loading constant, and increased the A:O molar ratio (9:1, 15:1) and reaction times (12 hours, 24 hours) but no conversion was observed. The reaction mixture was analyzed by GC upon completing the reactions, and showed no methyl ester peaks when compared to a chromatograph from a pure biodiesel sample. Furthermore, no noticeable reaction had occurred when the commercial sample of SnO was used under reaction conditions identical to those described above. With no other material in the literature or correspondence with the authors Abreu et al. (2005) to support the activity of SnO in transesterification reaction, further attempts to produce biodiesel with SnO as the catalyst ceased.

3.4 Sulfonated char synthesis and testing mthods

3.4.1 Sulfonated char synthesis procedure

Pyrolyzed hardwood char samples were obtained from Resource Transforms International Ltd. (Waterloo ON.), Ensyn Technologies Inc. (Ottawa, ON) and Dynamotiv Energy Systems Corp.

(Vancouver BC) and sulfonated according to the method of (Toda et al. 2005). 200 mL of concentrated sulfuric acid (98%, Sigma) were added to 20 g of char in a 500 mL round bottom flask. The mixture was heated to 150°C with a heating mantle (Fisher Scientific) and monitored with a temperature controller (Omega) and corrosion–resistant Type–J thermocouple (Omega) for 24 hours. After heating, the slurry was added to cool distilled water and then vacuum filtered through #40 Whatman filter paper. The char was washed with 80°C distilled water until the wash water was neutral and free from sulfate ions. Sulfate ions were tested for by precipitation by adding several drops of a 0.66 molar barium chloride solution to the wash water. Following filtration, the char was dried in an oven at 70°C for approximately 2 hours. Samples were characterized by the following techniques: surface area was measured using nitrogen adsorption at -196°C (Micromeritics ASAP 2000) and calculated with the single-point BET method; elemental composition was determined by elemental analysis (conducted by Canadian Microanalytical Services, Delta, British Columbia); catalyst structure was analyzed via X-ray diffraction (Rigaku Multiflex X-ray diffractometer, 2 kW); surface species bonded to the catalyst surface were determine by X-ray photon spectroscopy; the total and type of acidity of the catalyst were measured by pulse n-propylamine adsorption and temperature–programmed desorption, respectively; and scanning electron microscopy was used to assess the pore size of the catalysts. Three catalyst samples were prepared from three different char samples for catalytic testing. The char samples all originated from fast pyrolysis of the following feedstocks: Catalyst 1, hardwood (RTI); Catalyst 2, hardwoods and softwoods (Ensyn); Catalyst 3, wood waste, white wood, bark and shavings (DynaMotiv).

3.4.2 Sulfonated char testing procedure

The sulfonated char was tested for both transesterification and esterification activities in simple batch experiments. Reactions with canola oil were investigated to test Transesterification. Waste vegetable oil (from UBC Campus Food Outlets) was used to measure the esterification activity of the catalyst. Ethanol was used in order to achieve a higher reaction temperature (due to higher boiling point compared with methanol) and therefore faster reaction (Toda et al. 2005). Reactions were carried out on a hotplate with magnetic stirring under reflux at 76°C. The reaction mixture was analyzed by GC, as described in the Section 3.2.2. Esterification was quantified by measuring the acid number before and after the reaction. Samples were

centrifuged at 5000 rpm for 15 minutes to allow phase separation. The oil phase was then recovered by pipette and titrated for acid value using the Metrohm 794 Basic Titrino automatic titrator. Reactions were performed to determine the effect of reaction time and A:O molar ratio (3 hours, 9 hours and 15 hours; 3:1, 6:1 9:1, 12:1 and 15:1) , catalyst loading (1 wt.%, 2.5 wt.% and 5 wt.%), catalyst sample (Catalyst 1, 2 or 3) on the reduction in acid number.

3.5 Sulfonated char results and discussion

3.5.1 Catalyst characterization

3.5.1.1 BET surface area

The three catalyst samples were analyzed for surface area using nitrogen adsorption at -196°C to determine BET single point surface area as shown in Table 3.1. Each sample was tested in triplicate to test for reproducibility.

Table 3.1. BET surface areas for each catalyst sample.

Sample	Area (m^2/g)
Catalyst 1	5.84 ± 0.33
Catalyst 2	14.38 ± 1.55
Catalyst 3	2.74 ± 0.60

While the surface area among samples varies somewhat, they are all quite low as is typical for a bulk phase, unsupported catalyst. The surface area for Catalyst 1, which was synthesized from a hardwood derived sample of pyrolysis char is comparable to other surface area measurements reported for hardwood derived char (Della Rocca et al. 1999). The surface areas of the catalyst samples were all greater than that reported by Toda et al. (2005). This is likely due to the nature of the char substrate, which were all forms of wood biomass. The structure of the char had a highly complex network of pores, channels and otherwise fibrous ridged surfaces (observed from SEM photographs) as opposed to the planar structure of the sugar-derived char (Toda et al. 2005).

3.5.1.2 Elemental Analysis

Elemental analysis (presented in Table 3.2) revealed the composition of each catalyst sample by mass per cent, along with the corresponding molecular formula.

Table 3.2. Mass per cent composition by element and molecular formula of each catalyst sample.

Sample	C	H	N	O	S	Molecular Formula
Catalyst 1	68.12	2.77	0.11	28.73	2.12	$CH_{0.48}N_{0.001}O_{0.32}S_{0.011}$
Catalyst 2	55.17	2.72	0.23	31.62	1.71	$CH_{0.59}N_{0.004}O_{0.43}S_{0.008}$
Catalyst 3	70.81	2.34	0.13	20.28	1.83	$CH_{0.39}N_{0.001}O_{0.22}S_{0.009}$

The molecular formula reported by Toda et al. (2005) for their catalyst was $CH_{0.45}S_{0.01}O_{0.39}$, which, except for the nitrogen content in the samples presented here, is very close, indicating the catalysts presented here have similar compositions by mass.

3.5.1.3   X-Ray Diffraction Analysis

XRD experiments showed Catalyst 1 was an amorphous solid, similar to the catalyst reported by Toda et al. (2005). The XRD spectra for Catalyst 1 is presented in Figure 3.5. XRD spectra for Catalysts 2 and 3 also revealed amorphous structures.

3.5.1.4   XPS Analysis

XPS experiments were conducted to determine the surface species bonded to the catalyst carbon substrate. A broad survey scan was conducted between binding energies of 0 eV and 1350 eV. Narrow scans were then conducted in the S 2p region, C 1s region and the O 1s region. Figure 3.6 presents the survey scan for Catalyst 1, while Figures 3.7 and 3.8 present the narrow scans for the S 2p and C 1s regions, respectively. The narrow O 1s scan is not shown.

The peak in Figure 3.7 occurs at approximately 169 eV, which corresponds to the bonded sulfate groups (SO_4^{2-}). This is in contrast to the results reported by Toda et al. (2005), who indicated that SO_3H was the bonded sulfur species.

There are two peaks in Figure 3.8. The first, at 285 eV, corresponds to elemental carbon, which is the substrate of the catalyst. The second, (very small peak) observed in Figure 3.8 at 289 eV corresponds to carboxylic acid groups (COOH⁻) which is in agreement with the results of Toda et al. (2005) who also reported the presence of COOH⁻ groups.

3.5.1.5   n-Propylamine adsorption and temperature programmed desorption

Samples were tested for total acidity by pulse chemisorption experiments, and then subjected to a temperature programmed desorption (TPD) to determine the type of acid sites. Samples were

pretreated by holding the reactor temperature at 250°C for two hours in order to remove water and any adsorbed species. The sample temperature was then decreased to 120°C. After the thermal conductivity detector (TCD) readings had stabilized, the pulse experiments were conducted. The procedure was as follows. The sample loop was opened for two minutes, which allowed 1 mL of He gas containing 17.57 μmol of n-propylamine to fill the loop. At the end of the two minute period, the sample was injected into the reactor, and the outlet flow of n-propylamine measured by the TCD, logged by a multimeter (Fluke) and recorded by simple data logging software (FlukeView). After the baseline returned to an acceptable level (in all experiments the baseline was allowed to return to approximately 0.016 mV rather than 0.000 mV to reduce the length of the experiment) the sample loop was opened for two minutes and allowed to fill. The injection process was then repeated, until the peaks recorded appeared identical. In each experiment, nine pulse events were recorded. The adsorption peaks were integrated to determine the area of each one. Generally speaking, the first four of the nine peaks (Figure 3.9) of the analysis showed adsorption of the n-propylamine, while peaks 5 and beyond indicated that the catalyst sample was saturated, and therefore no n-propylamine was adsorbed.

The amount of n-propylamine adsorbed during peaks 1-4 was determined by dividing the area of each peak (from 1-4) by the average area of the saturated peaks. The total adsorption was found by adding the per cent adsorbed for peaks 1-4 and then divided by the sample mass to give a normalized value. After the pulse experiments, samples were allowed to sit for 1 hour at 120°C to remove any physisorbed species. The reactor temperature was then increased at a rate of 5°C/min to 700°C and then held for 30 minutes. The results of the pulse experiments are shown in Table 3.3 below.

Table 3.3. Total acidity for each catalyst sample.

Sample	Total acidity (μmol/g)
Catalyst 1	43.3
Catalyst 2	83.4
Catalyst 3	36.3

The total acidity of the catalysts presented here is much less than that reported by Toda et al. (2005), who achieved a total acidity of 1.4 mmol/g with the catalyst prepared from sulfuric acid. It is interesting to note however, that the acidity of the prepared catalysts is similar to the acidity

of the tungstated zirconia and sulfated zirconia (54 μmol/g and 94 μmol/g, respectively) tested by (Lopez et al. 2005).

The TPD curves for Catalysts 1 and 2 are presented in Figures 3.10 and 3.11, respectively. Each TPD curve follows the same pattern, and each peak occurs at approximately the same temperature, indicating that the types of acid sites on each catalyst are the same. Since the peaks occur at temperatures greater than 300°C, the acidity of the catalysts can be attributed entirely to Brønsted acid sites (Micromeritics 2003). The TPD curves were deconvoluted and four sub-peaks can be observed, numbered 1 to 4 on Figures 3.10 and 3.11. The solid line shows the TCD reading as a function of time (indicated on each TPD curve), while the dotted line shows the TCD reading as a function of temperature. The time-series curve has been deconvoluted. ·

Above 300°C the n-propylamine decomposes to propylene and ammonia. In the TPD analysis, the NH_3 peak lags the peak for propylene. Of the smaller peaks resulting from the deconvolution, the first two peaks (1 and 2, indicated on Figures 3.10 and 3.11) can be attributed to propylene and ammonia desorption, respectively, from a weak Brønsted acid site, which corresponds to the presence of $COOH^-$ groups as determined by XPS. The third and fourth peaks (numbered 3 and 4 on Figures 3.10 and 3.11) represent desorption of propylene and ammonia, respectively, from strong Brønsted acid sites, which correlates with the SO_4^{2-} groups observed in the XPS spectra for each catalyst. In order to check that the deconvolution gave a reasonable result, the ratio of the ammonia peak area divided by the propylene peak area can be calculated. Since propylene and ammonia are formed in equimolar amounts from the decomposition of n-propylamine, the peak areas for each species should be equal if the deconvolution of the TPD curve was done correctly. However, the thermal conductivity of ammonia is slightly greater than that of propylene (0.0409 and 0.0324 W/m.K, respectively); therefore the area of the ammonia peak should be larger by a factor of 1.26, i.e., the ratio of the thermal conductivities of the two species. Checking the area ratios for each set of peaks in Figure 3.10 gives ratios of 1.35 for peaks 1 and 2, and 1.13 for peaks 3 and 4, which are within 7% and 10% error, respectively, of the theoretical value of 1.26. For catalyst 2, the area ratios were 1.24 for peaks 1 and 2 (2% deviation) and 1.02 for peaks 3 and 4 (19% deviation). This indicates the results of the deconvolution are reasonable. With a reliable deconvolution, the relative amounts of each type of acid site can be determined by comparing the areas of the ammonia peaks. In the case of

50

Catalyst 1, the peak area for the strong acid sites was greater by approximately 17%, indicating the total acidity of the catalyst was skewed slightly in favour of the strong SO_4^{2-} sites. This is in contrast to the result reported by (Toda et al. 2005), indicating that 0.7 mmol/g of the total 1.4 mmol/g acidity could be attributed to the SO_3H groups incorporated into the catalyst. The TPD curve for Catalyst 2 (Figure 3.11) shows a higher proportion of weak acid sites. The TPD curve for Catalyst 3 (not shown) could not be satisfactorily deconvoluted; i.e.the ratio of peak areas for each pair of propylene and ammonia peaks was never satisfactorily close enough to the theoretical ratio of 1.26. This could be due to emission of volatile components within the char that are not present within the other two samples. In any case, no information regarding the distribution of active sites was ascertained for Catalyst 3.

3.5.1.6 SEM Experiments

Visual observation of the catalyst samples via SEM was performed to gain insight into catalyst morphology and pore size. All samples were observed with the same acceleration voltage of 20 kV. As shown in Figures 3.12 to 3.14, the catalyst samples have a highly irregular, convoluted fibrous surface structure, with little regular texturing. Discrete pores were visible in some images of Catalyst 1, (pore dimensions are indicated in the figure). However this was a rarity among the samples analyzed. The samples were also briefly investigated via energy dispersive X-ray analysis (EDX) to attempt to locate the active sites of the catalyst by analyzing the distribution of x-rays emitted by sulfur atoms upon excitement by the electron beam. However, the resolution of the EDX techniqued was not fine enough to pinpoint the location of the sulfur elements. Unfortunately, the SEM and EDX experiments yielded little insight into neither the nature and location of the catalyst active sites, nor the effect of catalyst morphology on catalytic activity.

3.5.2 Sulfonated char catalytic activity

Preliminary tests with the sulfonated char and canola oil (6:1 A:O ratio, 3 hours) indicated slight transesterification activity. GC analysis showed ethyl-ester peaks in the reaction mixture; however, the amount was too small to be accurately quantified. When the reaction was allowed to run for 24 hours at a higher A:O ratio (15:1), no visible increase in the amount of biodiesel produced was observed, although GC analysis showed the formation of some ethyl-esters, indicating there is some form of resistance to transesterification associated with the use of the sulfonated char.

Preliminary tests with waste vegetable oil collected from the UBC Biodiesel Pilot Plant were more favourable. The oil was analyzed for acid number before and after the reaction, and was found that at 12:1 A:O molar ratio and 3 hours, the acid number decreased from 8.5 mg KOH/g to 4.5 mg KOH/g. Additionally, qualitative transesterification activity was observed upon analysis of the reaction mixture by GC. Since the catalyst indicated favourable esterification properties, a set of screening experiments was conducted to determine the effect of A:O molar ratio, time and catalyst amount on ability of the catalyst to reduce the FFA present in the oil. Molar ratios investigated were 6:1, 9.5:1, 18:1, 28:1 38:1 and 48:1, and reaction time was changed between 3 h, 9 h and 15 h at a fixed catalyst amount of 5 wt.% based on the mass of waste vegetable oil. The range of molar ratios was selected based on the range of ratios tested in the literature (Furuta et al. 2004; Lopez et al. 2005; Jitputti et al. 2006). To determine the effect of catalyst amount on the reaction, catalyst loading was set at 1 wt.%, 2.5% and 5wt.% at a fixed A:O molar ratio of 28:1 and time of 3 hours.

Figure 3.15 shows the effect of reaction time at a fixed A:O molar ratio on the reduction in FFA. Except in the low molar ratio cases (6:1 and 9.5:1 reactions), increasing the reaction time allowed for a greater reduction in FFA content. The final acid number for both the 6:1 and 9.5:1 cases stayed relatively constant, which suggests that the reaction reaches equilibrium fairly quickly, and that increase in time does little to further drive the reaction forward. However, when the A:O molar ratio is increased to 18:1 and beyond, a significant drop in the final acid number can be observed, suggesting that the increased A:O molar ratio plays an important role in driving the equilibrium toward the products.

Above the 18:1 A:O molar ratio, there is only a slight difference between the final acid numbers that can be attributed to increased molar ratios, indicating that increasing the reaction time plays a greater role in the conversion of the FFA.

Figure 3.16 illustrates the effect of A:O molar ratio at fixed reaction time on the reduction in FFA. At low molar ratios, conversion of FFA is relatively low. However, it rapidly increases as the A:O molar ratio increases from 6:1 to 18:1, and begins to plateau with any further increases in A:O molar ratio. The error bars presented on the 15 hour trial give a sense of the variability

52

associated with the reaction and the quantification, and indicate that there might not be any quantifiable difference in the reduction in FFA when compared between the three reaction times, as the error bars overlap the other measurements. This has positive implications in an economic sense: since similar reaction conversion can be achieved in shorter times, this permits smaller reactor residence times, decreasing the size of the reactor; allowing for greater reactant throughput, both of which improve the economics of a production process as described by West et al. (2006).

Figure 3.17 presents the effect of A:O molar ratio on FFA conversion, specifically for the 15 hour reaction, to give a greater sense of the variability of the experiments. The curve clearly shows that increasing the A:O molar ratio to the maximum ratio investigated has an impact on the reduction in FFA. However, the variability of the 18:1, 28:1 and 38:1 measurements suggests that the improvement observed by increasing the A:O molar ratio beyond 18:1 may be difficult to accurately quantify.

Figure 3.18 illustrates the effect of catalyst amount on the conversion of FFA in the WVO. Increasing the catalyst amount in the reaction mixture increases the conversion of FFA. A greater amount of catalyst increases the number of active sites available for esterification which allows the reaction conversion to increase for a given amount of time. A similar effect on reaction conversion was observed by Kiss et al. (2006) for the esterification of oleic acid with sulfated zirconia.

Figure 3.19 presents the final acid number obtained at 28:1 A:O molar ratio, 5 wt.% catalyst after 3 hours for each catalyst sample. While Catalysts 1 and 3 performed relatively similarly under identical reaction conditions, it is curious that under the same reaction conditions Catalyst 2 could only achieve a final acid number of 1.94, i.e., double the final acid number in the Catalyst 1 and 3 reactions, especially in consideration of the higher total acidity of Catalyst 2. It is assumed that with a higher total acidity, there are a greater number of active sites available to the reactants on the catalyst, and therefore the more acidic catalyst would show greater activity. However, it may be that the type of site is an important influence on catalyst activity. Catalyst 2 indicated a higher proportion of weak acid sites (sites with the COOH⁻ species bonded) than did Catalyst 1, and if the weak acid sites do not catalyze the reaction as quickly or effectively (i.e.

the proton on the COOH⁻ group may be very slow to dissociate and attack the carboxyl group on the FFA) as the strong acid sites (SO_4^{2-}), this may account for the lesser activity observed with Catalyst 2.

It was also desired to test the catalyst for its ability to catalyze esterification reactions in a WVO with a very high FFA content. The sample of WVO used in the catalytic trials was spiked with a small amount of oleic-acid (Sigma) in order to increase the acid number of the WVO to 24.5 (approximately 12.25 wt.% FFA). The reaction was run at an alcohol-to-FFA molar ratio of 160:1 (Mbaraka and Shanks 2005), which translates to an A:O molar ratio of 78:1. Although these conditions are higher than what would be used in an industrial setting, they were chosen to provide a point of comparison to the highly complex catalyst prepared by Mbaraka and Shanks (2005). The catalyst loading was 5 wt.%, and the reaction time was 3 hours. In three separate trials, the acid number was reduced to an average value of 2.08 ± 0.19 mg KOH/g (roughly 1 wt.% FFA content). In contrast, the catalyst of Mbaraka and Shanks (2005) was able to reduce the amount of FFA in a 15 wt.% palmitic acid/soybean oil sample to approximately 2 wt.%. While the authors did not indicate the maximum amount of FFA content the catalyst could remain active under, it is clear that the catalyst prepared in this study performs comparably well to the catalyst prepared by Mbaraka and Shanks (2005), but with the advantage of requiring a considerably simpler method of preparation.

3.6   Conclusion

A study into the effectiveness of tin(II) oxide as a catalyst for the transesterification of vegetable oil was conducted. SnO was synthesized via the method of Fujita et al. (1990) after attempts to synthesize SnO using the procedure described by Abreu et al. (2005) failed. Both the synthesized sample and a commercial sample of SnO showed no catalytic activity during reactions run at 60°C with methanol and canola oil under reflux.

A second catalyst, sulfonated pyrolysis char, was synthesized based on the technique of Toda et al. (2005) et al. Characterization of the catalyst revealed an irregular, porous carbon framework with COOH⁻ and SO_4^{2-} groups bonded to the surface. The total acidity of the catalyst as revealed by pulse n-propylamine experiments (36 – 84 μmol/g) was similar to that reported by Lopez et al. (2005) for sulfated zirconia. Catalytic tests with canola oil and ethanol showed only qualitative transesterification. However, the catalyst was very active in the esterification of

FFAs. Experiments indicated that conversion of FFAs increased with increased reaction time, increased alcohol to vegetable oil molar ratio, and increased catalyst loading. It was found that at a catalyst loading of 5 wt.%, reaction time of 3 hours and A:O ratio of 18:1 gave the best results. Slight increases in FFA conversion were observed at molar ratios beyond 18:1 and reaction times of 9 hours and 15 hours, but the differences were not quantifiable due to the variability associated with the measurements. The catalyst was also tested for feeds with higher FFA concentrations. It was found that the catalyst was capable of reducing the amount of FFAs from 12.25 wt.% to approximately 1.04 wt.% (which corresponds to a decrease in acid number from 24.5 to 2.04 mg KOH/g), which was comparable with the highly complex mesoporous silica catalyst tested by (Mbaraka and Shanks 2005).

Sulfonated char shows considerable potential for use as a catalyst in biodiesel production, especially in a context used to reduce the free fatty acid content of a vegetable oil feedstock. However, for its true potential to be realized, the limitations to transesterification associated with this catalyst must be revealed and overcome. Future research will be directed toward this goal.

Figure 3.1. Sample of unknown substance obtained during SnO preparation via method of Abreu et al. (2005).
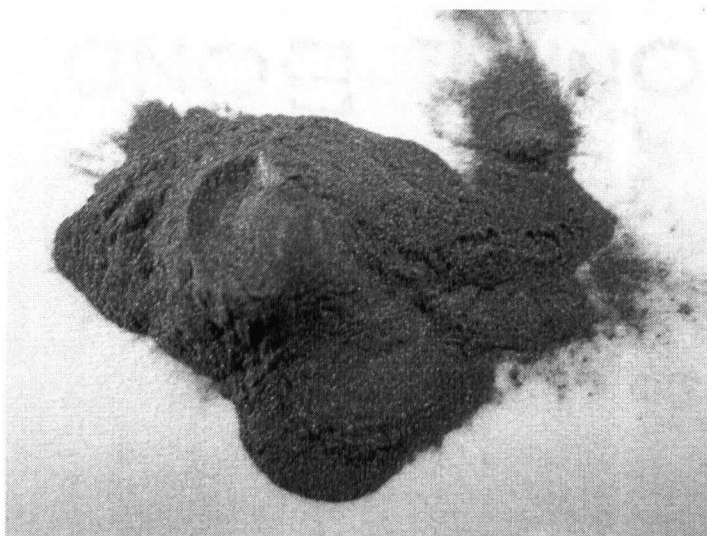
Figure 3.2. Commercial sample of SnO.
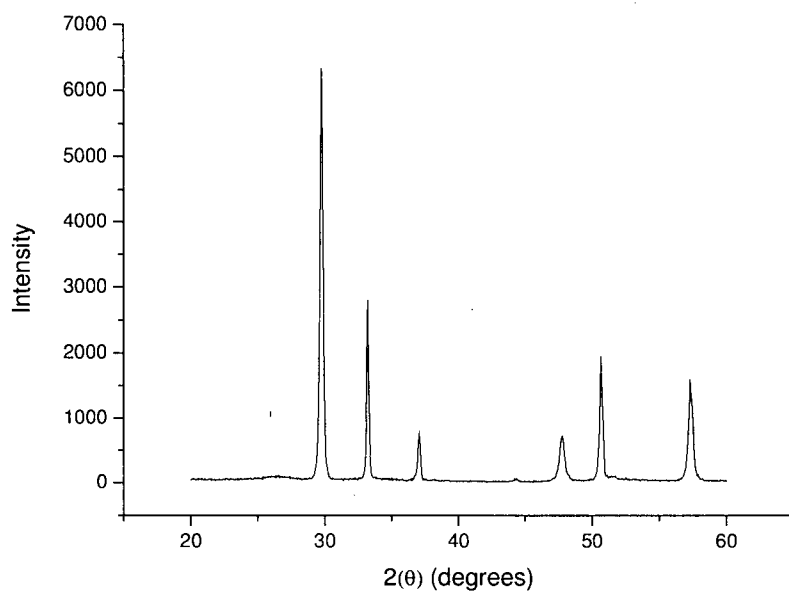
Figure 3.3. XRD pattern of SnO sample prepared by method of Fujita et al. (1990).
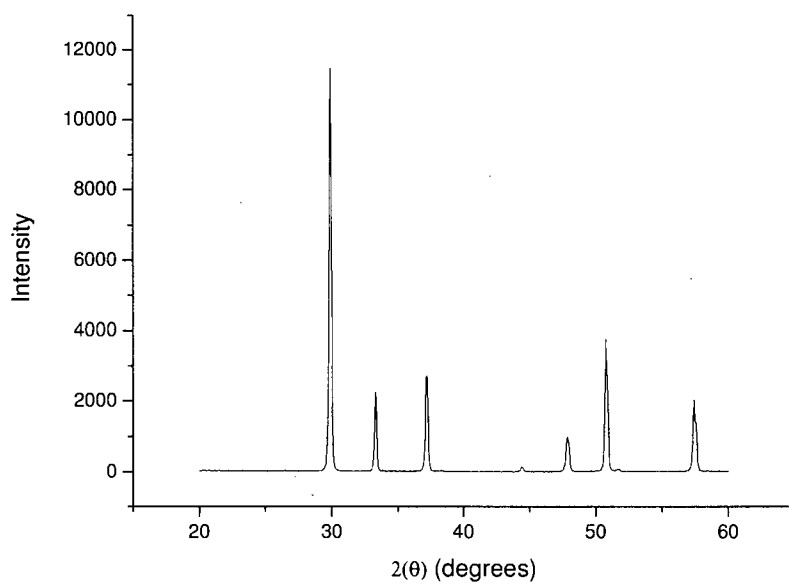
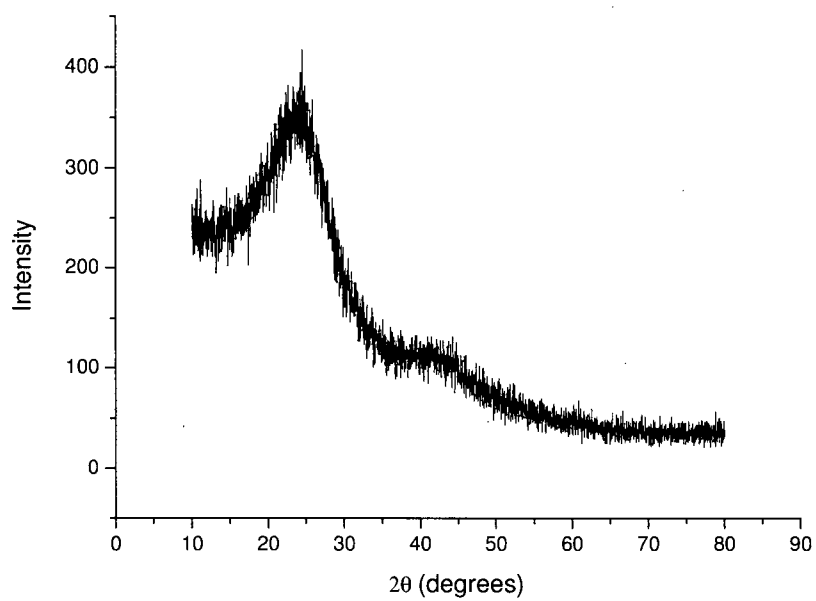

Figure 3.4. XRD pattern of commercial SnO sample.
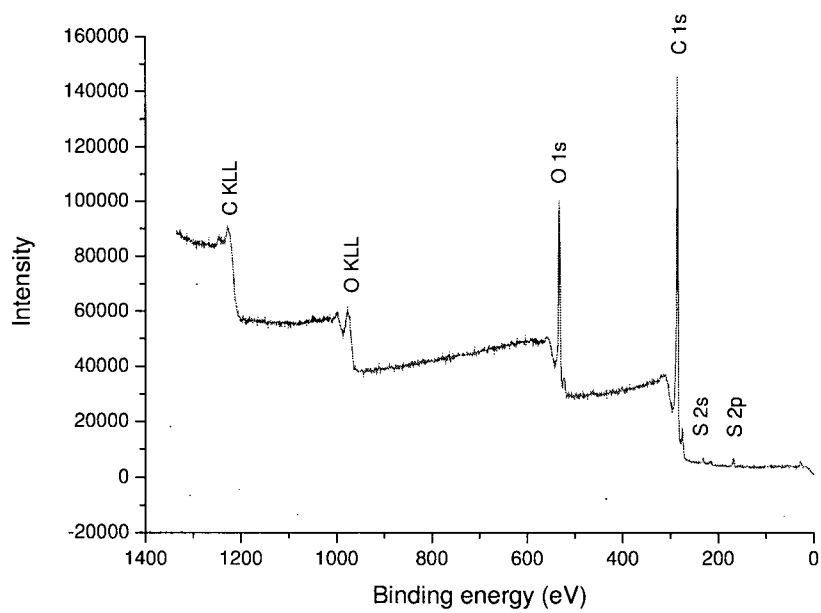
Figure 3.5. Catalyst 1 XRD pattern.
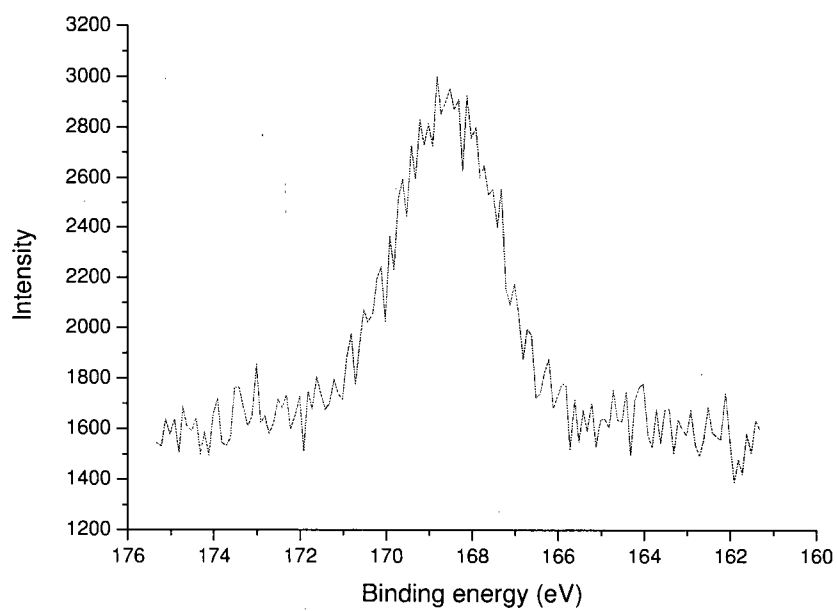

Figure 3.6. XPS survey scan for Catalyst 1.

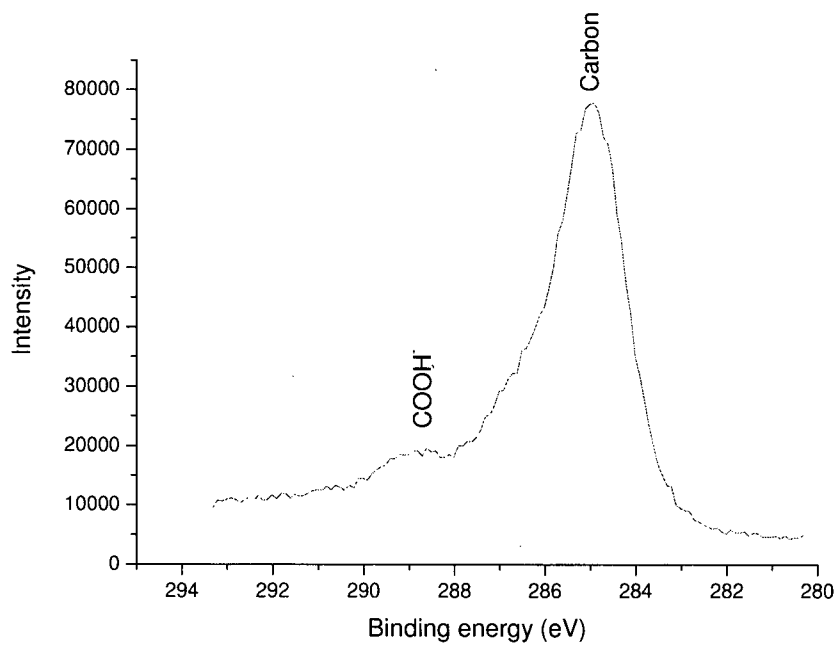**Figure 3.7.** Narrow scan in S 2p region for Catalyst 1.
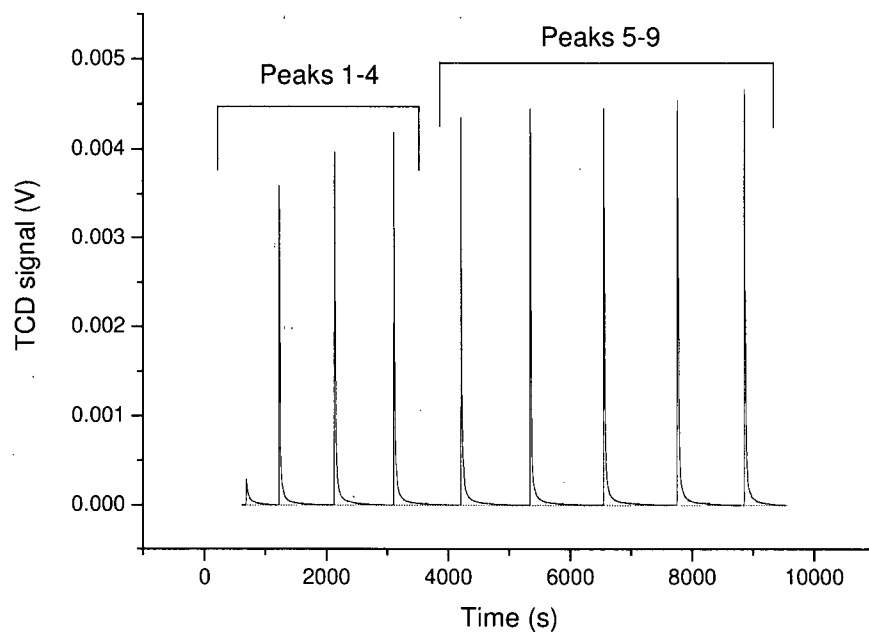

Figure 3.8. Narrow scan in C 1s region for Catalyst 1.

Figure 3.9. n-Propylamine pulse adsorption peaks for Catalyst 1.
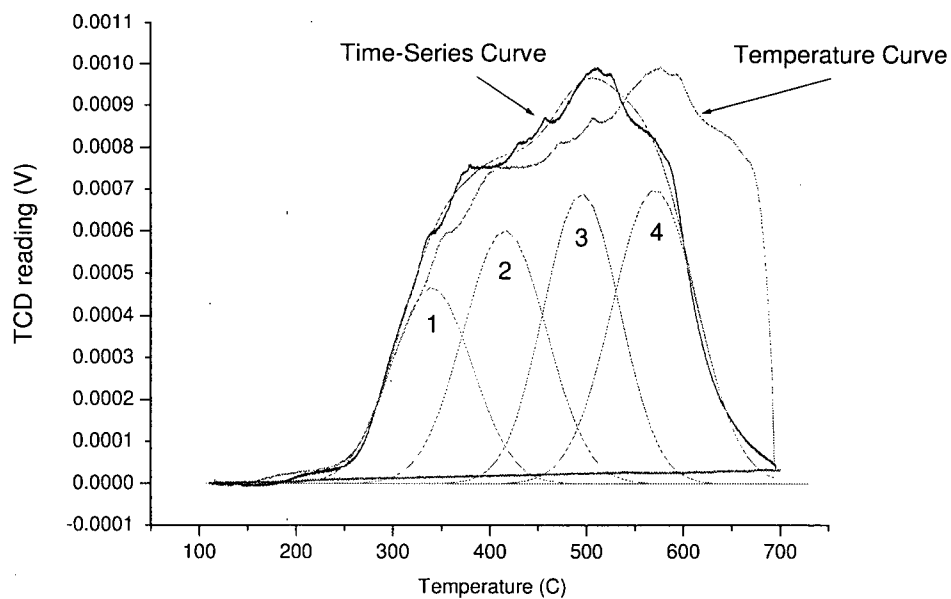
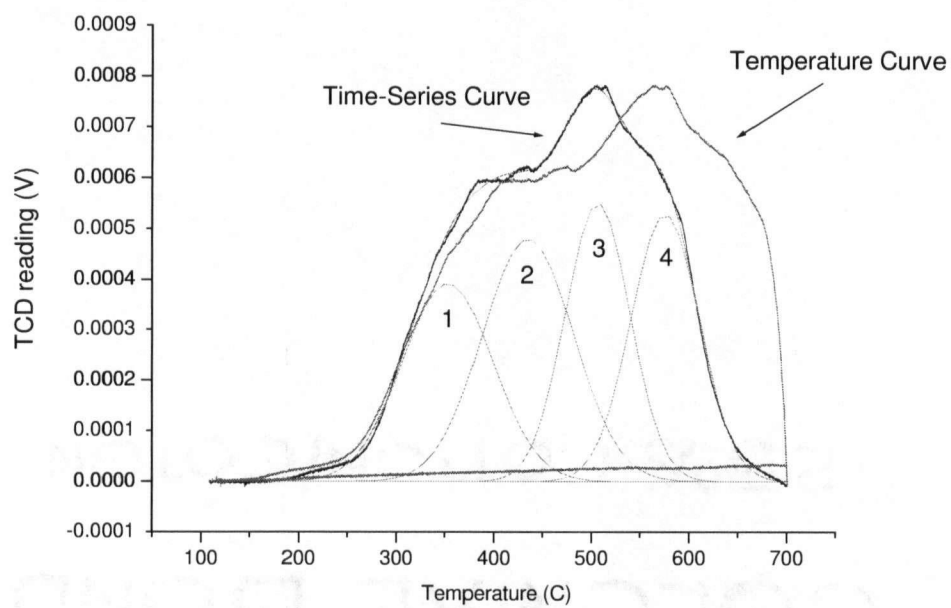**Figure 3.10.** TPD curve for Catalyst 1. Ratio of weak acid sites to strong acid sites is 0.85:1.

Figure 3.11. TPD curve for Catalyst 2. Ratio of weak acid sites to strong acid sites is 1.21:1.
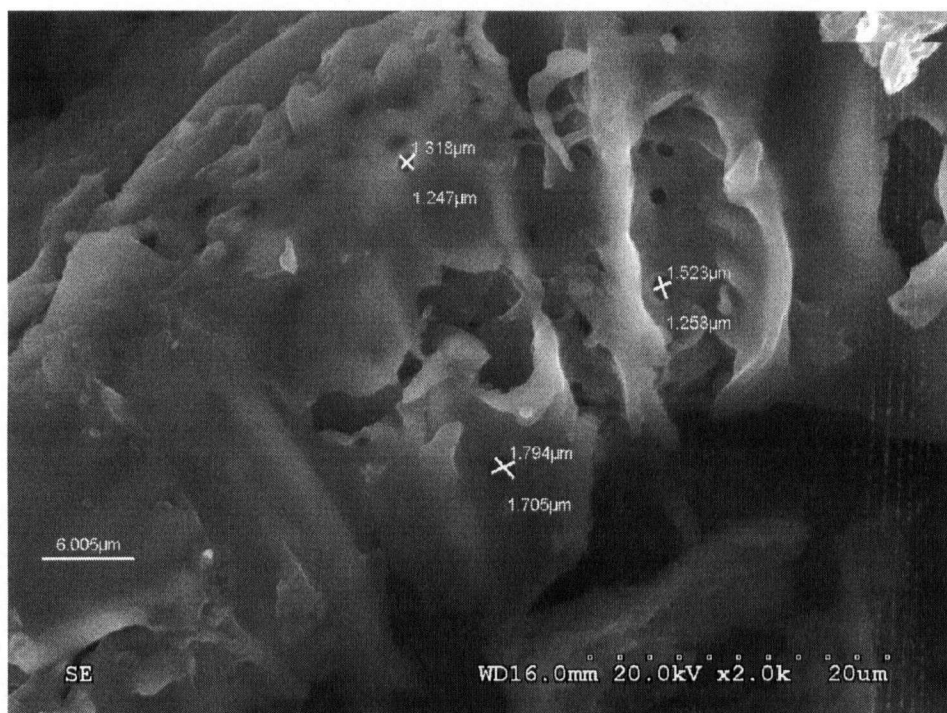

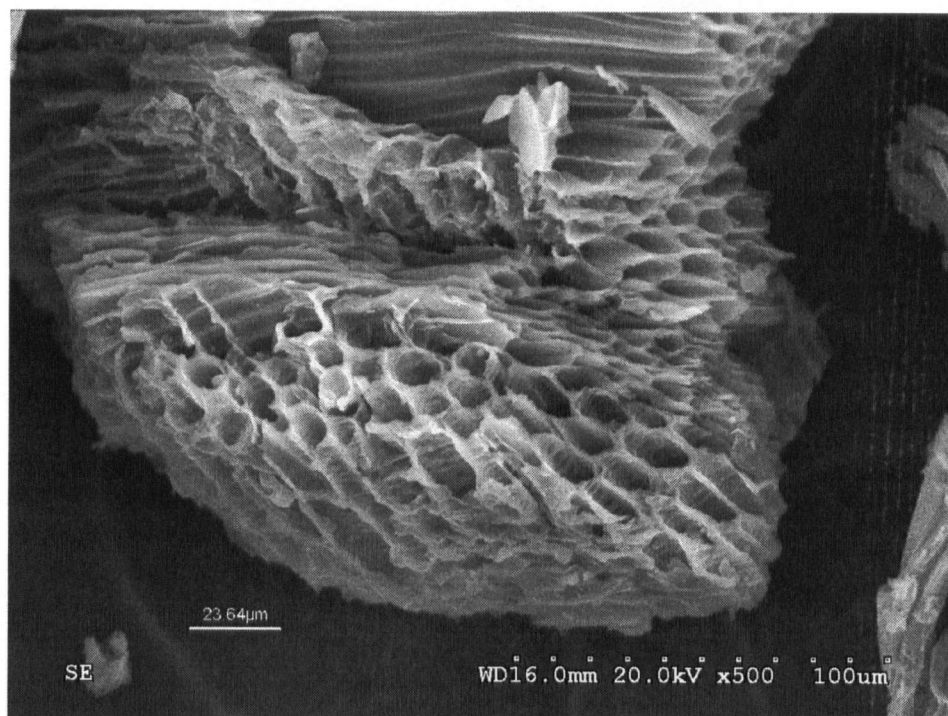**Figure 3.12** SEM image of Catalyst 1 indicating pore sizes.

Figure 3.13. SEM image of Catalyst 2 emphasizing fibrous channels and pore network.
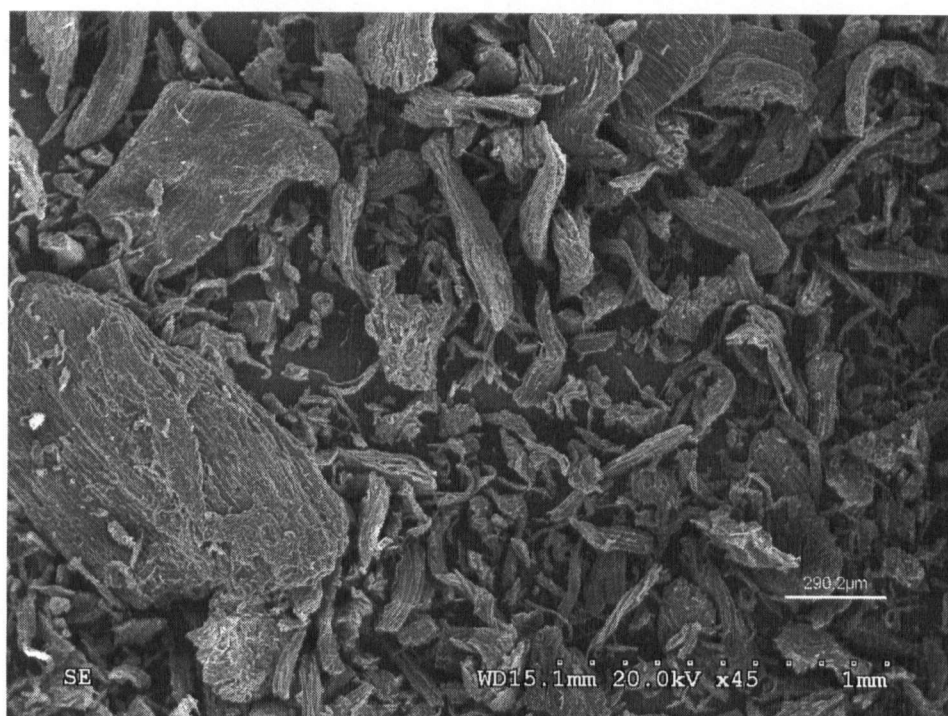

Figure 3.14. SEM image of Catalyst 3, highlighting variable size of catalyst particles.
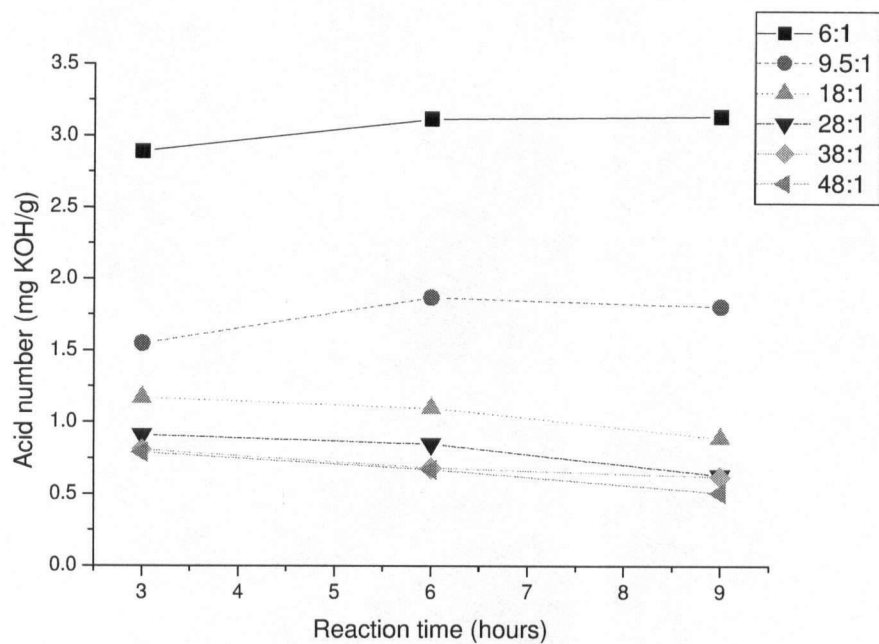
Figure 3.15. Effect of reaction time on final acid number. Reactions were run at 5 wt.% catalyst 1 with ethanol at A:O molar ratios of 6:1, 9.5:1, 18:1, 28:1, 38:1, 48:1.
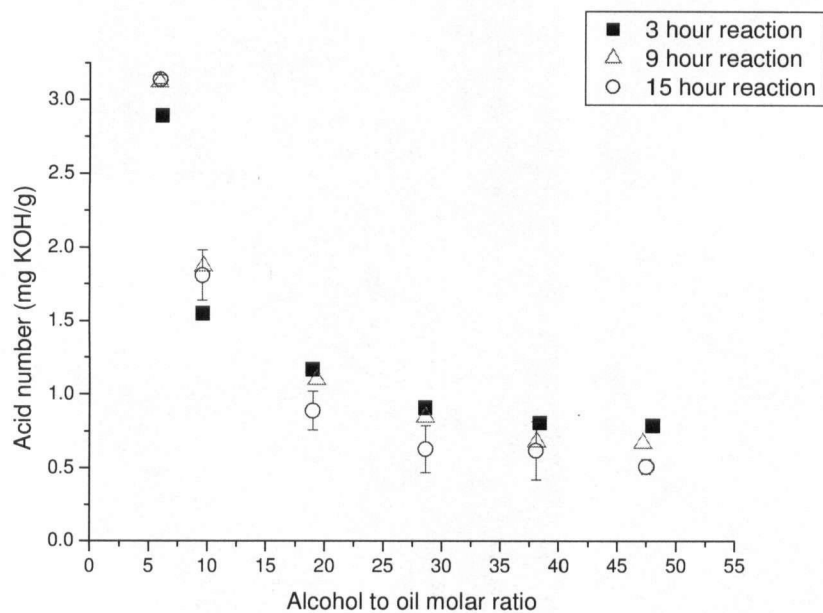

Figure 3.16. Effect of A:O molar ratio at fixed reaction time on final acid number. 5 wt.% catalyst 1.
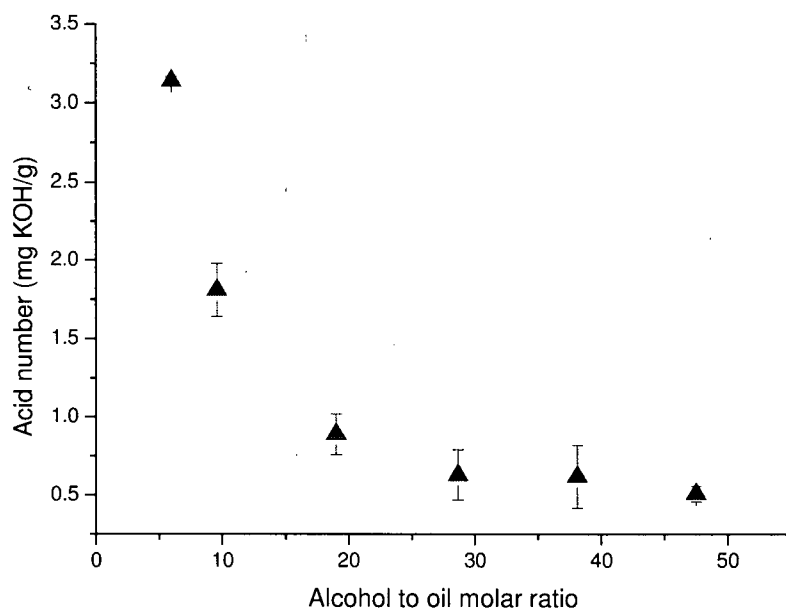
Figure 3.17. Effect of A:O molar ratio on final acid number for the 15 hour set of reactions. 5 wt.% Catalyst 1
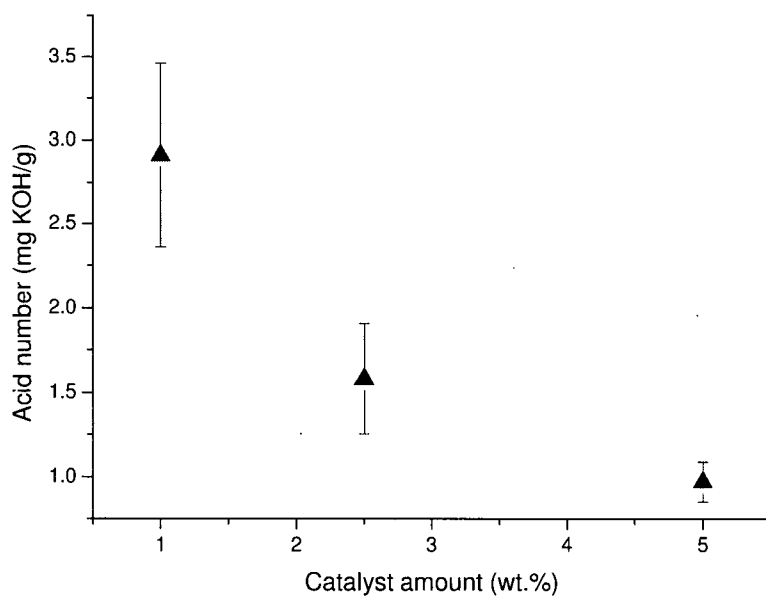

Figure 3.18. Effect of catalyst amount on final acid number. 28:1 A:O molar ratio, ethanol, 5 wt.% catalyst 1.
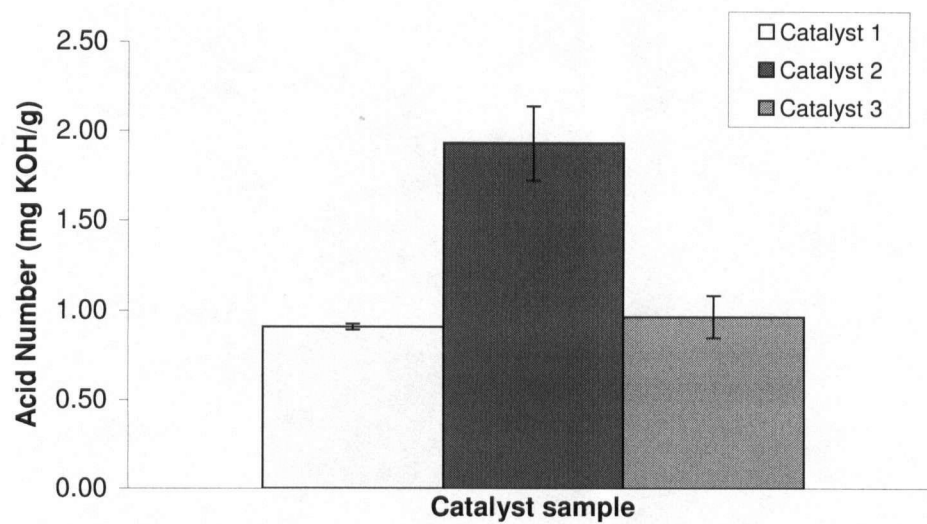
Figure 3.19. Final acid number of reaction mixture after reaction with each catalyst sample. 3 hour reaction, 28:1 A:O molar ratio, 5 wt.% catalyst loading

3.7 References

Abreu, F. R., Alves, M. B., Macedo, C. C. S., Zara, L. F. and Suarez, P. A. Z. (2005). New multi-phase catalytic systems based on tin compounds active for vegetable oil transesterification reaction. Journal of Molecular Catalysis A: Chemical 227(1-2): 263-267.

Bridgwater, A. V., Meier, D. and Radlein, D. (1999). An overview of fast pyrolysis of biomass. Organic Geochemistry 30(12): 1479-1493.

Canakci, M. and Van Gerpen, J. (1999). Biodiesel production via acid catalysis. Transactions of the ASAE 42(5): 1203-1210.

Della Rocca, P. A., Cerrella, E. G., Bonelli, P. R. and Cukierman, A. L. (1999). Pyrolysis of hardwoods residues: on kinetics and chars characterization. Biomass and Bioenergy 16(1): 79-88.

Dynamotiv Dynamotiv - Technology - Feedstocks. http://www.dynamotive.com/biooil/feedstocks.html (July 20, 2006),

Freedman, B., Pryde, E. H. and Mounts, T. L. (1984). Variables Affecting the Yields of Fatty Esters from Transesterified Vegetable-Oils. J. Am. Oil Chem. Soc. 61(10): 1638-1643.

Fujita, K., Nakamura, C., Matsuda, K. and Mitsuzawa, S. (1990). Preparation of tin(II) oxide by a homogeneous precipitation method. Bulletin of the Chemical Society of Japan 63(9): 2718-2720.

Furuta, S., Matsuhashi, H. and Arata, K. (2004). Biodiesel fuel production with solid superacid catalysis in fixed bed reactor under atmospheric pressure. Catalysis Communications 5(12): 721-723.

Holbein, B. E., Stephen, J. D. and Layzell, D. B. (2004). Canadian Biodiesel Initiative: Aligning Research Needs and Priorities With the Emerging Industry. Ottawa ON, BIOCAP Canada Foundation: 1-35.

Jitputti, J., Kitiyanan, B., Rangsunvigit, P., Bunyakiat, K., Attanatho, L. and Jenvanitpanjakul, P. (2006). Transesterification of crude palm kernel oil and crude coconut oil by different solid catalysts. Chemical Engineering Journal (Amsterdam, Netherlands) 116(1): 61-66.

Kiss, A. A., Dimian, A. C. and Rothenberg, G. (2006). Solid acid catalysts for biodiesel production - towards sustainable energy. Advanced Synthesis & Catalysis 348(1 + 2): 75-81.

Krawczyk, T. (1996). Biodiesel. INFORM 7(8): 801-822.

Lopez, D. E., Goodwin, J. G., Bruce, D. A. and Lotero, E. (2005). Transesterification of triacetin with methanol on solid acid and base catalysts. Applied Catalysis, A: General 295(2): 97-105.

Lotero, E., Liu, Y. J., Lopez, D. E., Suwannakarn, K., Bruce, D. A. and Goodwin, J. G. (2005). Synthesis of biodiesel via acid catalysis. Ind. Eng. Chem. Res. 44(14): 5353-5363.

Mbaraka, I. K. and Shanks, B. H. (2005). Design of multifunctionalized mesoporous silicas for esterification of fatty acid. J. Catal. 229(2): 365-373.

Micromeritics (2003). Application Note 134 - Characterization of Acid Sites Using Temperature-Programmed Desorption.

Saka, S. and Kusdiana, D. (2001). Biodiesel fuel from rapeseed oil as prepared in supercritical methanol. Fuel 80(2): 225-231.

Toda, M., Takagaki, A., Okamura, M., Kondo, J. N., Hayashi, S., Domen, K. and Hara, M. (2005). Green chemistry: Biodiesel made with sugar catalyst. Nature (London, United Kingdom) 438(7065): 178.

Tyson, K. S. Biodiesel: Handling and Use Guidelines. http://www.eere.energy.gov/biomass/pdfs/biodiesel_handling.pdf (November 28, 2004).

Warabi, Y., Kusdiana, D. and Saka, S. (2004). Reactivity of triglycerides and fatty acids of rapeseed oil in supercritical alcohols. Bioresource Technology 91(3): 283-287.

West, A. H., Posarac, D. and Ellis, N. (2006). Assessment of four biodiesel production processes using hysys.Plant. Bioreseource Technology (Submitted for publication February 2006).

Zhang, Y., Dube, M. A., McLean, D. D. and Kates, M. (2003). Biodiesel production from waste cooking oil: 2. Economic assessment and sensitivity analysis. Bioresource Technology 90(3): 229-240.

4 Conclusion, General Discussion and Recommendations

4.1 General discussion

Chapter 2 featured four continuous processes to produce biodiesel at a rate of 8000 tonnes/year that were designed and simulated in HYSYS.Plant, with the aim of conducting an economic evaluation to determine which process yielded the most cost effective means of producing biodiesel. As previously mentioned, the component triolein was unavailable in the HYSYS databanks, and therefore had to be created. Certain parameters were imported from the ASPEN Plus databanks where triolein was available as a component. However, one key set of parameters, the Antoine's coefficients were not available in ASPEN Plus and therefore had to be estimated in HYSYS. ASPEN Plus was used to double check the results of the HYSYS Antoine's coefficient estimation, by using ASPEN Plus to estimate its own set of Antoine's coefficients and then graphing the vapour pressure as a function of temperature. Doing so revealed something of an anomaly. At low temperatures, it was found that the vapour pressure curve for triolein crossed that of glycerol and methyl-oleate, indicating it had a higher vapour pressure, which was completely unexpected. It was expected that such a large molecule would have a much lower vapour pressure. Using the HYSYS Antoine's coefficients to produce a vapour pressure curve revealed the same phenomena. A review of the literature was undertaken to obtain vapour pressure data for triolein in order to more accurately predict the Antoine's coefficients. Unfortunately, the data were either too limited or were unsatisfactory and therefore unsuitable for use. In light of the situation, the parameters estimated by HYSYS were assumed to be the best available and used for the simulation. While it is desirable to use the most accurate correlation possible simply for the sake of correctness, correct parameters will also improve the simulation results, by giving a more accurate simulation of the methyl-oleate/triolein separation in the second distillation column. Assuming that HYSYS is overpredicting the vapour pressure for triolein, this will result in high temperatures required to separate the two components, increasing the energy consumption and therefore the cost of the process. Of course, the opposite case holds true as well. Fortunately, this potential error does not affect the relative economic standing of each process. Since the material flows through the relevant distillation column are all approximately equal, the error in terms of energy consumption (and therefore cost) will all be skewed to approximately the same degree, leaving the standings unaltered.

Another important consideration is whether the failure to reproduce the results of Abreu et al. (2005) invalidate the conclusion that the heterogeneous process would be the most economical. To that end, a second catalyst, sulfated zirconia (SO_4^{2-}/ZrO_2) was used in the simulation. A number of researchers have confirmed the ability of SO_4^{2-}/ZrO_2 to catalyze the transesterification of vegetable oils (Furuta et al. 2004; Lopez et al. 2005; Jitputti et al. 2006). The reaction conditions investigated by Jitputti et al. (2006) were adopted for the simulation, as they were they most rigorous in terms of temperature and pressure. The result of the simulation showed that in spite of the increased cost of the unit operations necessary for handling the large material flows and withstanding the high pressure and temperature required for the reaction, the heterogeneous process was still the most economical, although the after tax rate of return was significantly reduced from 54% in the SnO catalyzed process to 24%. This part of the work is currently in preparation for presentation at the 1st International Congress on Green Process Engineering in Toulouse France (2007).

Based on the result from Chapter 2, Chapter 3 detailed the work that was undertaken to synthesize SnO, and then test it to assess its catalytic abilities under a variety of conditions. Unfortunately, both the commercial SnO sample obtained and the SnO sample synthesized displayed no activity during the reaction of canola oil with methanol. Discussion with Mr. J. Radlein with reference to the work of Toda et al. (2005) brought about the idea to test sulfonated pyrolysis char for transesterification acivity. Testing of the sulfonated char at an A:O molar ratio of 18:1 with ethanol at 76°C under reflux for 24 hours showed no visible signs of transesterification, but analysis of the reaction mixture via GC indicated the presence of some ethyl-ester. The chromatogram (not shown) also exhibited peaks associated with glycerol, di-glycerides and mono-glycerides, which would not be present if the ethyl-ester was being produced exclusively through esterification of any free fatty acids present in the oil. Due to time constraints the limitations to transesterification could not be explored. There are a number of possibilities that could explain the lack of transesterification acitivity. The first is that the catalyst may not have been acidic enough. However, the total acidity measured for the sulfonated char was comparable to the acidity of sulfated zirconia reported by Lopez et al. (2005), and the activity of sulfated zirconia is well confirmed. Catalytic studies have also shown that internal resistance to mass transfer and stearic hindrance can also limit catalyst activity when microporous catalysts are used, such as Zeolite Hβ (pore size 5.5 Å x 5.5 Å), H-ZSM5

and Y (Lopez et al. 2005; Kiss et al. 2006) and that in such cases any activity was the result of surface sites. SEM experiments were conducted to assess the surface characteristics of the catalyst, but no regularly occurring pore structures could be observed. Where they were found (Figure 3.12) the surface pore size was quite large (>1.6 µm) which would not present any resistance to diffusion. However, some form of mass transfer resistance may be limiting activity, if perhaps the active sites were all within the long fibrous channels observed in Figure 3.13. To assess whether the active sites were located on the surface of the catalyst or within the pores/channels, an EDX scan was performed to locate the S-containing sites. Unfortunately the resolution was not fine enough to pinpoint the location of the sulfur and no information regarding the location of the active sites could be gained.

Another possibility may have been that the reaction temperature was too low for transesterification to occur. Other studies (Furuta et al. 2004; Suppes et al. 2004; Jitputti et al. 2006) have used much higher temperatures (>150°C), than could be achieved with the simple hotplate set-up employed for this work. Nonetheless, if temperature is the limiting factor, it is expected that some transesterification would be observed at lower temperatures (Lopez et al. 2005).

4.2 Conclusions

Using the HYSYS simulator, process flowsheets and energy and material balances were developed to model the processes. The integrated spreadsheet tool in HYSYS was used to conduct unit operation sizing, as well as automate the economic calculations, which included all equipment costing, total capital investment, total manufacturing cost and after tax rate of return. The processes were as follows: (I) a homogeneous alkali-catalyzed process that used pure vegetable oil as the feedstock; (II) a homogeneous acid-catalyzed process that converted waste vegetable oil as the feedstock; (III) a heterogeneous acid-catalyzed process that used waste vegetable oil; and (IV) a supercritical non-catalyzed process, that consumed waste vegetable oil. The supercritical process was the simplest and had the fewest number of unit operations, while the homogeneous processes had the greatest number of unit operations, and were the most complicated, owing to the difficulty in removing the catalyst from the liquid phase.

An economic assessment revealed that the heterogeneous acid-catalyzed process had the lowest total capital investment and total manufacturing cost. It was found that raw materials consumed and the size of material flows, strongly affected process economics. Accordingly, Processes II,

70

III and IV had much lower manufacturing costs than Process I. The after tax rate of return for process III was 54%, while processes I, II and IV had rates of return of –144%, –4% and –0.9%, respectively.

Sensitivity analyses were conducted to identify any unit operations where operating specifications could be modified to improve the process. It was found that increasing methanol recovery led to a greater ATROR. Accordingly, methanol recovery was set as high as possible (>99%) before the glycerol degradation temperature (150°C) was exceeded in the homogeneous acid-catalyzed and supercritical processes. Use of the optimizer function indicated a vacuum system could be installed in the HAC process to increase methanol recovery and consequently the ATROR, while keeping the bottoms stream within the temperature limit. An analysis of the effect of reaction conversion on ATROR revealed that even at reduced reaction conversion (i.e., between 85-93%) , the ATROR of the HAC process is greater than at 100% conversion of the homogeneous acid and supercritical processes. Therefore Process III, the heterogeneous acid-catalyzed process, is clearly advantageous over the other processes, as it had the highest rate of return, lowest capital investment, and technically, was a relatively simple process. Further research in developing the heterogeneous acid-catalyzed process for biodiesel production is warranted.

Based on the results from the HYSYS simulation, a study into the effectiveness of tin(II) oxide as a catalyst for the transesterification of vegetable oil was conducted. SnO was synthesized via the method of Fujita et al. (1990) after attempts to synthesize SnO using the procedure described by Abreu et al. (2005) had failed. Both the synthesized sample and a commercial sample of SnO showed no catalytic activity during reactions run at 60°C with methanol and canola oil under reflux.

A second catalyst, sulfonated pyrolysis char, was synthesized based on the technique of Toda et al. (2005) et al. Characterization of the catalyst revealed an irregular, porous carbon framework with $COOH^-$ and SO_4^{2-} groups bonded to the surface. Catalytic tests with canola oil and ethanol showed only qualitative (i.e., an amount too small to be physically measured) transesterification. However, the catalyst was very active in the esterification of FFAs. Experiments showed that conversion of FFAs increased with increasing reaction time, increasing alcohol to vegetable oil

molar ratio, and increasing catalyst loading. It was found that at a catalyst loading of 5 wt.%, reaction time of 3 hours and A:O ratio of 18:1 gave the best results. Slight increases in FFA conversion were observed at molar ratios beyond 18:1 and reaction times of 9 hours and 15 hours, but the differences were not quantifiable due to the variability associated with the measurements. At higher FFA concentrations, it was found that the catalyst was capable of reducing the amount of FFAs from 12.25 wt.% to approximately 1.04 wt.%. Sulfonated char shows considerable potential for use as a catalyst in biodiesel production, especially in a context used to reduce the free fatty acid content of a vegetable oil feedstock. However, for its true potential to be realized, the limitations to transesterification associated with this catalyst must be revealed and overcome. Future research will be directed toward this goal.

4.3   Recommendations

Based on the work conducted for this thesis, a number of recommendations are proposed to for future research.

- The estimation of the Antoine's coefficients in HYSYS needs to be improved. It is therefore suggested that experiments designed to measure the vapour pressure of triolein (or vegetable oil) be conducted at the temperature range of interest, between 25°C to 400°C. The Antoine coefficients can then be obtained by regressing the data, and then input into the process simulations.

- Experiments should also be performed to verify that the 3-phase separator used in Processes III and IV to remove glycerol can achieve the results of the simulations.

- The simulated feedstocks could be expanded to include those with FFA contents greater than 5 wt.%, as in the case of yellow grease, and high water contents. Such factors may change the relative economic order of the processes.

- Since the heterogeneous process indicated such promising results, it would also be of interest to conduct a more detailed simulation, where more care is taken to optimize the distillation columns. It would also be desirable to include kinetic information (i.e., the effects of temperature and residence time) in the reactor modelling to give a more realistic representation of the system.

- It is also recommended that the reasons for the failure of SnO to catalyze any reaction should be investigated, as well as why the method of Abreu et al. (2005) failed. Since the ATROR of the heterogeneous process drops dramatically from 54% to 24% when

sulfated zirconia is used, it be economically advantageous to use the SnO catalyzed process.

With respect to the sulfonated char, it is very important to understand and overcome the limitations to transesterification associated with the catalyst and experiments should be designed to elucidate the problems.

- Synthesis of the catalyst with fuming sulfuric acid has been shown to increase the total acidity (Toda et al. 2005), which may have an effect on the reaction. It is recommended that catalytic trials be conducted with char treated with fuming sulfuric acid.

- The char utilized in this study exhibited a highly complex, irregular network of pores and fibrous channels, which may pose mass internal mass transfer limitations on the large triglyceride molecules. Char obtained from the pyrolysis of coal has shown a less convoluted, highly regular porous structure (Yu et al. 2004) when compared to the char utilized in this study. Testing of a catalyst derived from coal char could yield some insight into any resistance that mass transfer might play.

- Alternately, it is possible that the lack of catalyst transesterification activity is due to external mass transfer limitations. If ethanol binds to the active sites (perhaps through hydrogen bonding), that could prevent the non-polar triglycerides from accessing the active sites and being protonated by the acid groups. In the case of FFA conversion, the polar carboxylic acid group of the FFA could still access the active site, allowing the reaction to occur. Using a cosolvent to create one oil/alcohol phase could overcome any potential external mass transfer limitations, and therefore allow the reaction to occur.

- To determine if reaction temperature is the limitation, it is recommended to test the reaction with the catalyst at elevated temperatures.

- A number of studies to examine the performance of the sulfonated char in the esterification reaction would also be useful: investigating the effect of feedstock water content on the reaction; determining the maximum amount of FFAs in the feedstock before the reaction is inhibited; and testing the catalyst's reusability.

- Lastly, determination of kinetic parameters for the esterification and transesterification reactions would be very valuable. Such data would enhance the simulation for Process III, and be very important for the scale-up of the reaction to an industrial scale.

4.4 References

Abreu, F. R., Alves, M. B., Macedo, C. C. S., Zara, L. F. and Suarez, P. A. Z. (2005). New multi-phase catalytic systems based on tin compounds active for vegetable oil transesterification reaction. Journal of Molecular Catalysis A: Chemical 227(1-2): 263-267.

Fujita, K., Nakamura, C., Matsuda, K. and Mitsuzawa, S. (1990). Preparation of tin(II) oxide by a homogeneous precipitation method. Bulletin of the Chemical Society of Japan 63(9): 2718-2720.

Furuta, S., Matsuhashi, H. and Arata, K. (2004). Biodiesel fuel production with solid superacid catalysis in fixed bed reactor under atmospheric pressure. Catalysis Communications 5(12): 721-723.

Jitputti, J., Kitiyanan, B., Rangsunvigit, P., Bunyakiat, K., Attanatho, L. and Jenvanitpanjakul, P. (2006). Transesterification of crude palm kernel oil and crude coconut oil by different solid catalysts. Chemical Engineering Journal 116(1): 61-66.

Kiss, A. A., Dimian, A. C. and Rothenberg, G. (2006). Solid acid catalysts for biodiesel production - towards sustainable energy. Advanced Synthesis & Catalysis 348(1 + 2): 75-81.

Lopez, D. E., Goodwin, J. G., Bruce, D. A. and Lotero, E. (2005). Transesterification of triacetin with methanol on solid acid and base catalysts. Applied Catalysis, A: General 295(2): 97-105.

Suppes, G. J., Dasari, M. A., Doskocil, E. J., Mankidy, P. J. and Goff, M. J. (2004). Transesterification of soybean oil with zeolite and metal catalysts. Applied Catalysis a-General 257(2): 213-223.

Toda, M., Takagaki, A., Okamura, M., Kondo, J. N., Hayashi, S., Domen, K. and Hara, M. (2005). Green chemistry: Biodiesel made with sugar catalyst. Nature 438(7065): 178.

Yu, J. L., Harris, D., Lucas, J., Roberts, D., Wu, H. W. and Wall, T. (2004). Effect of pressure on char formation during pyrolysis of pulverized coal. Energy & Fuels 18(5): 1346-1353.